Table 1. Recovery of standard glycosylated proBNP and BNP added to human plasma.

Added peptide concentration, pmol/L	Recovery, %	Recovery, %
	proBNP assay system	total BNP assay system
2.0	90	85
25.0	101	97
100.0	95	95

doi:10.1371/journal.pone.0053233.t001

Antibodies

The monoclonal antibodies BC203 (IgG1, k) and KY-BNP-II (IgG1, k) were developed by Shionogi & Co., Ltd [10]. BC203 and KY-BNP-II recognize the C-terminal region and the ring region of BNP, respectively. The monoclonal antibody 18H5 was purchased from Hytest Ltd. 18H5 recognizes a region (a.a. 13–20) of proBNP. In the proBNP assay, the combination of BC203 (capture) and 18H5 (detection) was used because 18H5 is not affected by glycosylation [11]. In the total BNP assay, the combination of BC203 (capture) and KY-BNP-II (detection) was used because KY-BNP-II recognizes nearly all bioactive BNPs (Figure 1).

Preparation of BC203 coated immunoassay plates

BC203, which was the capture antibody in both assays, was biotinylated using an EZ-Link-sulfo-NHS-biotinylation kit according to the manufacturer's instructions. The biotinylated BC203 (0.2 mg/well in 100 mL PBS) was added to streptavidin-coated plates and incubated for 18 h at 4°C. After washing with a saline containing 0.01 g/dL Tween 20 and 0.05 g/dL sodium azide (Wash Buffer), the BC203 coated immunoassay plates were dried in a desiccator.

Preparation of 18H5 (Fab')-ALP and KY-BNP-II (Fab')-ALP

The 18H5 and KY-BNP-II mAbs (IgG) were digested with pepsin (IgG/pepsin = 1/0.05) for 4 h at 37°C in 100 mM citrate buffer (pH 4.0) containing 100 mM NaCl. Thereafter, Fab' solution was prepared by reduction with 10 mM 2-mercaptoethylamine in 0.1 M phosphate buffer (pH 6.0) containing 5 mM EDTA using the standard method [12]. Alkaline phosphatase from calf intestine (ALP; 2.0 mg or 14.2 nmol; Kikkoman, Chiba, Japan) in 0.475 mL 0.1 M Tris-HCl buffer (pH 7.0) containing 1 mM MgCl2 and 0.1 mM ZnCl2 was mixed with 31 mg (71 nmol) of Sulfo-HMCS in 0.05 mL of water for 1.5 h on ice, after which the HMCS-activated ALP was purified on a PD-10 column (GE Healthcare, Chalfont St. Giles, UK). Aliquots of HMCS-activated ALP solution (0.96 mg in 0.192 mL) were each added to 0.441 mg of the Fab' in 0.15 mL of 0.1 M phosphate buffer (pH 6.0) containing 5 mM EDTA and mixed for 16 h at 4°C. Unlabeled Fab' antibody was removed using a TSKgel 3000SWxl column. The purified 18H5 (Fab')-ALP and KY-BNP-II (Fab')-ALP were then diluted with a StabilZyme AP (BioFX Lab.) and stored at 4°C until use.

Sandwich 2-step Chemiluminescent Enzyme Immunoassay

After the BC203 coated immunoassay plates were washed with a wash buffer, 50 mL of test sample or calibrator and 50 mL of Assay Buffer (0.05 M Tris-HCl buffer (pH 7.4), 1 g/dL BSA, 0.01 g/dL Tween80, 1 mM MgCl2, 0.1 mM ZnCl2, 1000K IU/mL Aprotinin, 0.1 mg/mL mouse gamma globulin, 0.9 g/dL NaCl) were added to the wells. The plates were then incubated for 3 h at 25°C. After washing with wash buffer, 100 mL of detection antibodies (18H5 (Fab')-ALP, 100 ng/ml; KY-BNP-II (Fab')-ALP, 416 ng/ml) were added to the wells. The plates were then incubated for 1 h at 25°C, followed by washing with wash buffer and addition of substrate (CDP/E) solution. The chemiluminescence from each well was then measured using a plate reader (Wallac 1420 Arvo sx, Perkin Elmer, Inc., MA).

Study Patients

We collected blood samples from heart failure patients (18 men and 14 women; age range, 34–84 years, mean age, 65±11 years) hospitalized at Kyoto University Hospital. The primary causes of the heart failure were ischemic heart disease (n = 8), cardiomyopathy (n = 8), valvular heart disease (n = 7), pulmonary hypertension (n = 7) and others (n = 2), which were diagnosed from the medical history, physical examination and chest radiographic, electrocar-

Table 2. Effects of dilution on recovery rates with the proBNP and total BNP assay systems.

Dilution magnitude	proBNP assay system		total BNP assay system	
	Measured, pmol/L	Recovery, %	Measured, pmol/L	Recovery, %
1	94	-	95	-
2	105	112	101	107
5	96	102	104	109
10	92	98	92	97
20	97	103	93	98
50	99	105	97	103
100	87	92	95	100

doi:10.1371/journal.pone.0053233.t002

Table 3. Intra- and Inter-assay precision of the proBNP assay systems.

	Added proBNP concentration pmol/L	Measured concentration pmol/L		CV	Bias
		Mean	S.D.	%	%
Intra-assay (n = 5)	2.0	2.0	0.2	8.0	2.0
	25	25	1.3	5.2	0.0
	100	101	5.5	5.4	1.0
Inter-assay (n = 15)	2.0	1.9	0.1	5.3	−5.8
	25	23	1.7	7.4	−8.0
	100	96	6.1	6.4	−4.0

doi:10.1371/journal.pone.0053233.t003

diographic, echocardiographic and/or cardiac catheterization findings. Patients with symptomatic heart failure were under medication, including angiotensin-converting-enzyme inhibitors/angiotensin-receptor blockers, digitalis and diuretics. The New York Heart Association (NYHA) functional classes were class I–II (n = 19) and class III–IV (n = 13). Healthy subjects (61 men and 54 women; age range, 30–78 years, mean age, 50±10 years) were selected based on their normal physical, laboratory, chest radiographic, electrocardiographic and echocardiographic findings, and their BNP levels.

Plasma samples

Blood samples were drawn into plastic syringes and quickly transferred to chilled tubes containing EDTA (1.5 mg/mL, blood) and aprotinin (500 U/mL blood) and centrifuged at 1600× g for 20 min at 4°C. The obtained plasma samples were stored at −80°C until assayed.

Assay of plasma NT-proBNP levels

Plasma levels of NT-proBNP were measured using Elecsys proBNP II assay system (Roche Diagnostics, Basel, Switzerland).

Gel filtration chromatography

Plasma samples were extracted using Sep-Pak C18 cartridges (Waters, Milford, MA, USA) as previously described [6]. The eluate was lyophilized and dissolved in 30% acetonitrile containing 0.1% TFA. The resultant solution (300 ml) was separated by gel filtration HPLC on a Superdex 75 10/300 GL columns (10×300 mm×2, GE Healthcare) in the same buffer at a flow rate of 0.4 mL/min. The column effluent was fractionated every minute into polypropylene tubes containing bovine serum albumin (100 mg) and each fraction was analyzed using the total BNP and proBNP assay systems. Because recent studies have shown that glycosylated proBNP with a MW of about 30 K circulates in the plasma [7], we examined the gel filtration positions at which commercial recombinant proBNP and glycosylated proBNP, and synthetic BNP were eluted to determine which is the major molecular form of BNP in human plasma.

Deglycosylation enzyme treatment

We further analyzed the immunoreactive proBNP levels to determine whether immunoreactive proBNP in plasma is glycosylated. Eluate lyophilized after extraction on a Sep-Pak C18 column was dissolved in phosphate buffer and incubated with or without a cocktail of deglycosylation enzymes for 24 h at 37°C, as previously described [13]. The enzyme cocktail included O-glycosidase (Roche Diagnostic) and neuraminidase (Roche Diagnostics) at final concentrations of 4.25 and 42.5 mU/mL, respectively. These two enzymes were essential for the deglycosylation, and the enzyme concentrations and incubation period were selected based on the results of preliminary and previously reported studies [11,13,14]. We then lyophilized the sample again and dissolved it in 30% acetonitrile containing 0.1% TFA, after which it was subjected to gel-filtration HPLC as described above.

Statistical Analysis

All values are expressed as means ± SD. The statistical significance of differences between 2 groups was evaluated using Fisher's exact test or unpaired Student's t test, as appropriate. Variables were compared among three groups using one-way analysis of variance followed by Bonferroni's multiple comparison

Table 4. Intra- and Inter-assay precision of the total BNP systems.

	Added BNP concentration pmol/L	Measured concentration pmol/L		CV	Bias
		Mean	S.D.	%	%
Intra-assay (n = 5)	2.0	2.3	0.2	7.0	15.0
	25	25	2.1	8.4	1.0
	100	99	7.1	7.2	−0.7
Inter-assay (n = 15)	2.0	2.1	0.2	9.5	5.0
	25	24	1.7	2.9	−4.0
	100	100	1.9	1.9	0.0

doi:10.1371/journal.pone.0053233.t004

Table 5. Cross-reactivity between proBNP and BNP.

Added peptide concentration, pmol/L	Added peptide concentration, pmol/L	Measured peptide concentration, pmol/L	Measured peptide concentration, pmol/L
proBNP	BNP	proBNP assay	total BNP assay
50	50	58	114
100	10	113	119
10	100	8	113

doi:10.1371/journal.pone.0053233.t005

test. Correlation coefficients were calculated using linear regression analysis. Values of $P<0.05$ were considered significant.

Results

Standard curve, recovery and precision

Figure 2 shows typical standard curves for the proBNP and total BNP assay systems. The lower detection limits were 0.04 pmol/L (proBNP) and 0.02 pmol/L (total BNP). At these levels the mean value (n = 8 each) of the chemiluminescence intensity (cps) was more than twice that at 0 pmol/L ($P<0.05$). The working range (coefficient of variation (CV)<15%) of both assays was 0.2–250 pmol/L in total BNP and 0.4–250 pmol/L in proBNP, respectively.

Table 1 shows the recovery of standard proBNP and BNP, which was estimated from the levels of glycosylated proBNP or BNP added to clinically available plasma (endogenous total BNP = 0.3 pmol/L and proBNP = 0.2 pmol/L). In the proBNP assay system, using glycosylated proBNP as a standard, the recovery ranged from 90–101%. In the total BNP assay system, using BNP as the standard the recovery ranged from 85–97%. The effect of diluting plasma samples containing 100 pmol/L glycosylated proBNP or BNP is shown in Table 2. At every dilution level, the recovery rate was good. We also investigated the effects of dilution on plasma levels of total BNP and proBNP in three heart failure patients. As shown in Figure 2B, the calculated total BNP and proBNP values varied linearly with dilution (correlation coefficients = 0.998–1.00).

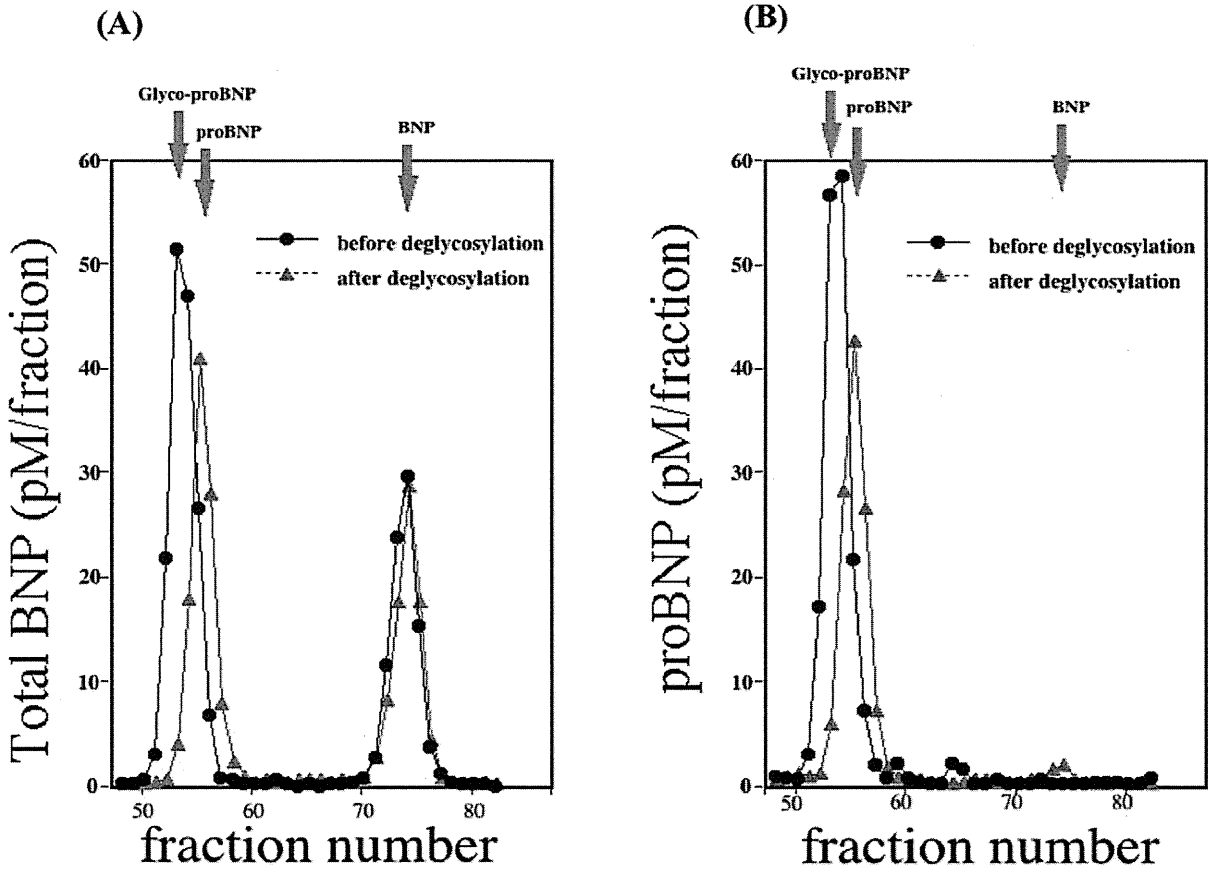

Figure 3. Gel filtration analysis of total BNP (A) and proBNP (B) in plasma from a heart failure patient. Fractions were assayed using the total BNP (A) and proBNP (B) systems. The elution points for glycosylated proBNP, proBNP and BNP are indicated by red arrows. Black and red lines respectively show gel filtration analyses of total BNP (A) and proBNP (B) in the same plasma sample before and after deglycosylation.
doi:10.1371/journal.pone.0053233.g003

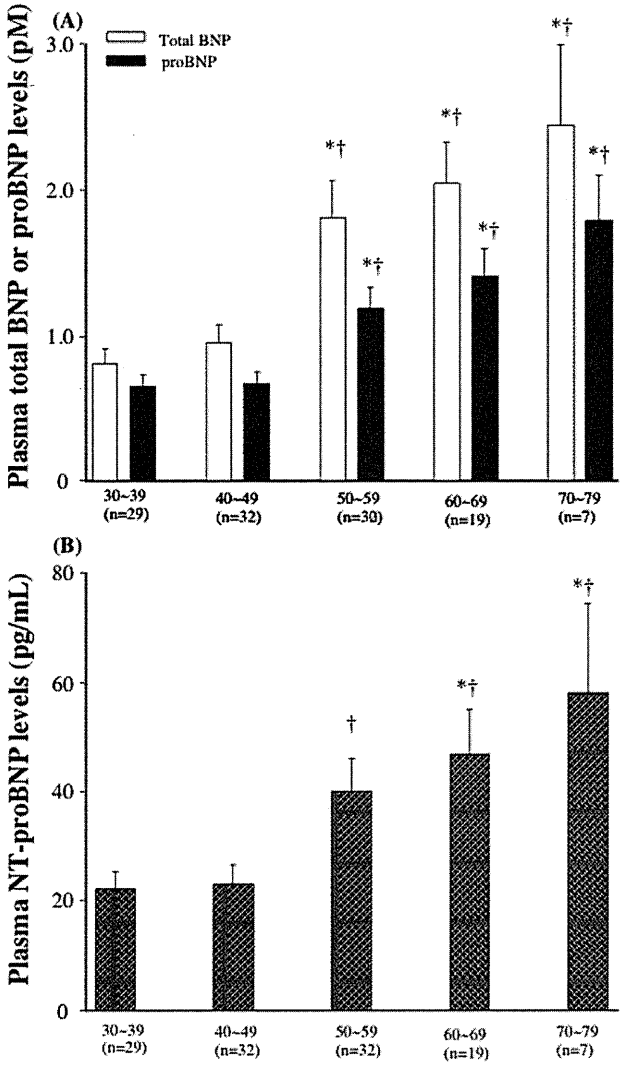

Figure 4. Plasma Levels of total BNP, proBNP, and NT-proBNP in different age groups. Bar graph showing the total BNP, proBNP (A) and NT-proBNP levels (B). Values are means ± SE., *P<0.05 vs total BNP, proBNP, and NT-proBNP in 30~39, †P<0.05 vs total BNP, proBNP, and NT-proBNP in 40~49.
doi:10.1371/journal.pone.0053233.g004

When we then assessed the intra- and inter-assay precision using plasma spiked with glycosylated proBNP or BNP, we found that the intra-assay CV ranged from 5.2%–8.0% in proBNP assay and from 7.0%–8.4% in total BNP assay, while inter-assay CV ranged from 5.3–7.4% in proBNP assay and from 1.9%–9.5% in total BNP assay, respectively (Table 3, 4).

Specificity and sensitivity

We next examined the cross-reactivity between proBNP and BNP. As shown in Table 5, the presence of BNP did not affect the values measured with the proBNP assay system. Moreover, the values measured with the total BNP assay system were the sum of the BNP and proBNP even at different compositions of these two peptides. Thus, the total BNP assay recognized both BNP and proBNP with the same efficiency and sensitivity. Likewise, the proBNP and total BNP assay systems recognized proBNP with the same efficiency and sensitivity.

Gel-filtration chromatography before and after deglycosylation procedure

Figure 3-A shows two immunoreactive BNP peaks detected using the total BNP assay with HPLC fractions. The first peak appeared in fractions 52–55 and the second peak in fractions 72–75. With the same sample, one immunoreactive BNP peak was detected by the proBNP assay (Figure 3-B); the position of that peak was completely consistent with the proBNP peak obtained with the total BNP assay. When subjected to gel filtration HPLC, recombinant proBNP, glycosylated proBNP and BNP were eluted mainly in fractions 53, 56 and 74, respectively. Treating the same plasma sample with an enzyme cocktail catalyzing deglycosylation shifted the first peak to fraction 54–56, which is consistent with the proBNP peak. From these results, we conclude that total BNP assay evaluates the sum of the glycosylated proBNP plus BNP, while proBNP assay detects glycosylated proBNP. The proBNP was not detected in a significant level with either assay system.

Plasma concentrations of proBNP, total BNP, and NT-proBNP in healthy subjects and heart failure patients

Plasma total BNP, proBNP and NT-proBNP levels in different age groups were shown in Figure 4-A, B. Plasma total BNP, proBNP and NT-proBNP levels appeared to increase according to the age. The older age groups (more than 50) had higher total BNP, proBNP and NT-proBNP levels than younger age groups (less than 50); however, there were no statistical differences in NT-proBNP between 30~39 and 50~59. In addition, there were significant positive relationships between plasma total BNP ($r = 0.467$, $p<0.001$), proBNP ($r = 0.491$, $p<0.001$) and NT-proBNP ($r = 0.376$, $p<0.001$) levels and age (Figure 5-A, B, C).

The mean total BNP and proBNP in plasma from 116 healthy subjects were 1.4±1.2 pM and 1.0±0.7 pM, respectively (Figure 6-A). Female had higher total BNP than male (total BNP: 1.7±1.3 vs 1.1±1.1, $P<0.05$; proBNP: 1.1±0.8 vs 0.8±0.6 pM, $P = 0.11$) (Figure 6-C). proBNP/total BNP ratio was lower in female than that in male. NT-proBNP was also higher in female than those in male (Figure 6-E). The total BNP and proBNP levels were markedly elevated in heart failure patients, and the magnitude of the increase reflected the severity of the patients' condition as observed in NT-proBNP (Figure 6-A, B).

Discussion

Plasma levels of the cardiac hormone BNP increase in proportion to the severity of heart failure. Indeed, plasma BNP levels are used as a biomarker of heart failure, and the guidelines in many countries recommend that BNP be used as a diagnostic indicator of acute and chronic heart failure [1–3]. The stimuli that increase cardiac BNP production include pressure overload, volume overload and ischemia, as well as various cytokines and neurohumoral factors [15]. In response to these stimuli, BNP mRNA expression is rapidly upregulated. Following translation of the protein, the signal peptide is removed to produce proBNP, which is then cleaved into BNP and the NT-proBNP fragment during secretion [15]. It is noteworthy that BNP and proBNP could not be distinguished from one another in earlier BNP assay systems because the anti-BNP antibodies cross-reacted with proBNP. We therefore endeavored to develop a new assay system that would enable separate measurement of BNP and proBNP. Recent studies have shown that levels of uncleaved proBNP are increased in heart failure to a greater degree than BNP [5–7,16]. Using a combination of gel filtration and an immunoenzyme fluorescent assay for BNP, we previously found that proBNP levels are increased in heart failure and that the proBNP/total BNP

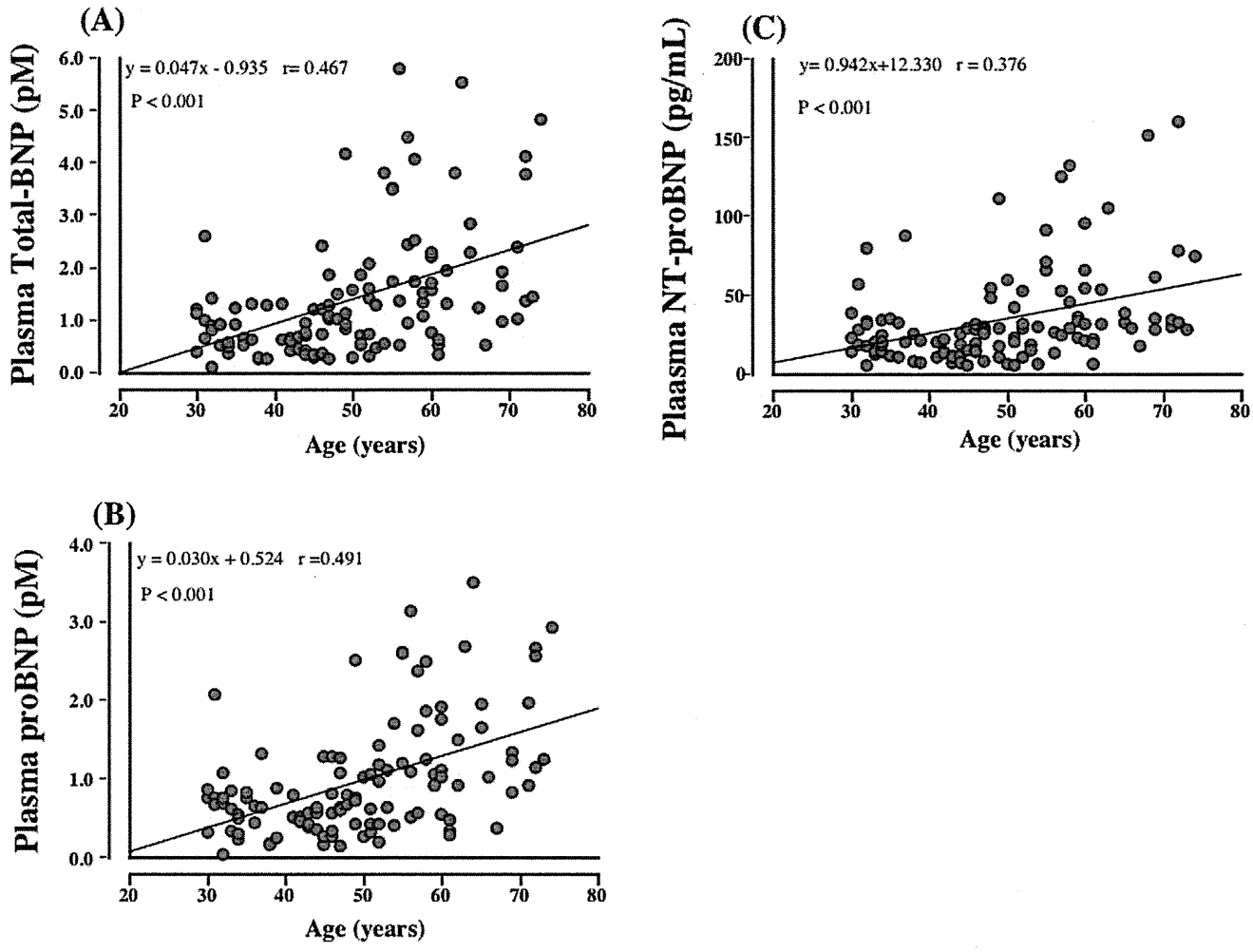

Figure 5. The relationships between total BNP (A), proBNP (B), and NT-proBNP (C) and age.
doi:10.1371/journal.pone.0053233.g005

ratios are higher in heart failure patients with ventricular overload than those with atrial overload [6]. Although this protocol provides useful information, the methodology is time-consuming and impractical for routine assays in clinical laboratories. In addition, recovery of proBNP may be diminished by both extraction and the gel filtration steps [9,16]. To overcome these problems, we developed new direct immunochemiluminescent assays for proBNP and total BNP.

We used two monoclonal antibodies, BC203 and 18H5, to assay proBNP. BC203 recognizes an epitope in the C-terminal of proBNP, while 18H5 recognizes an epitope in the N-terminal. Recent studies showed that proBNP has seven sites suitable for *O*-linked oligosaccharide attachment (Ser36, Thr37, Thr44, Thr48, Thr53, Ser58 and Thr71) within the N-terminal portion of the peptide [14]. Because the *O*-linked oligosaccharide attachments almost completely inhibit the binding of the antibody to the peptide [17], we selected 18H5, which recognizes the N-terminal of proBNP (a.a. 13–20) in a region not subject to glycosylation (Figure 1). To assay total BNP, we used the monoclonal antibodies BC203 and KY-BNP-II, as previously reported [10]. In both assays, BC203 served as the capture antibody. Importantly, because the affinity of 18H5 for the N-terminal portion is similar to the affinity of KY-BNP-II for the ring structure, we are able to calculate the proBNP/total BNP ratio. In addition, our new assays are less time-consuming and more sensitive and accurate than earlier ones, and the lower detection limits for total BNP (0.02 pmol/L) and proBNP (0.04 pmol/L) enabled us to measure plasma proBNP levels in nearly all the healthy subjects tested.

We used gel-filtration on two tandemly connected Superdex 75 columns to determine the molecular mass of plasma proBNP. As shown in Figure 3-A,B, a single peak of proBNP was obtained in both the total BNP and proBNP assay systems. The elution points are consistent with that of glycosylated proBNP, but not deglycosylated proBNP, and deglycosylation treatment significantly shifted the peak rightward (Figure 3-A,B) to an elution point consistent with proBNP. The peak immunoreactivity of proBNP after deglycosylation was slightly smaller than before treatment, suggesting the recovery rate of proBNP after gel-filtration is lower than that of glycosylated proBNP, which is consistent with proBNP being more adsorptive than glycosylated proBNP. Our findings are also consistent with previous Western blot analyses showing that plasma levels of glycosylated proBNP are elevated and no substantial level of proBNP is detected in severe heart failure [7]. Taken together, these results suggest that the major molecular form of proBNP in the plasma of patients with heart failure is the glycosylated form.

ProBNP is also the important molecular form of BNP in the plasma of healthy subjects. When we previously used gel-filtration

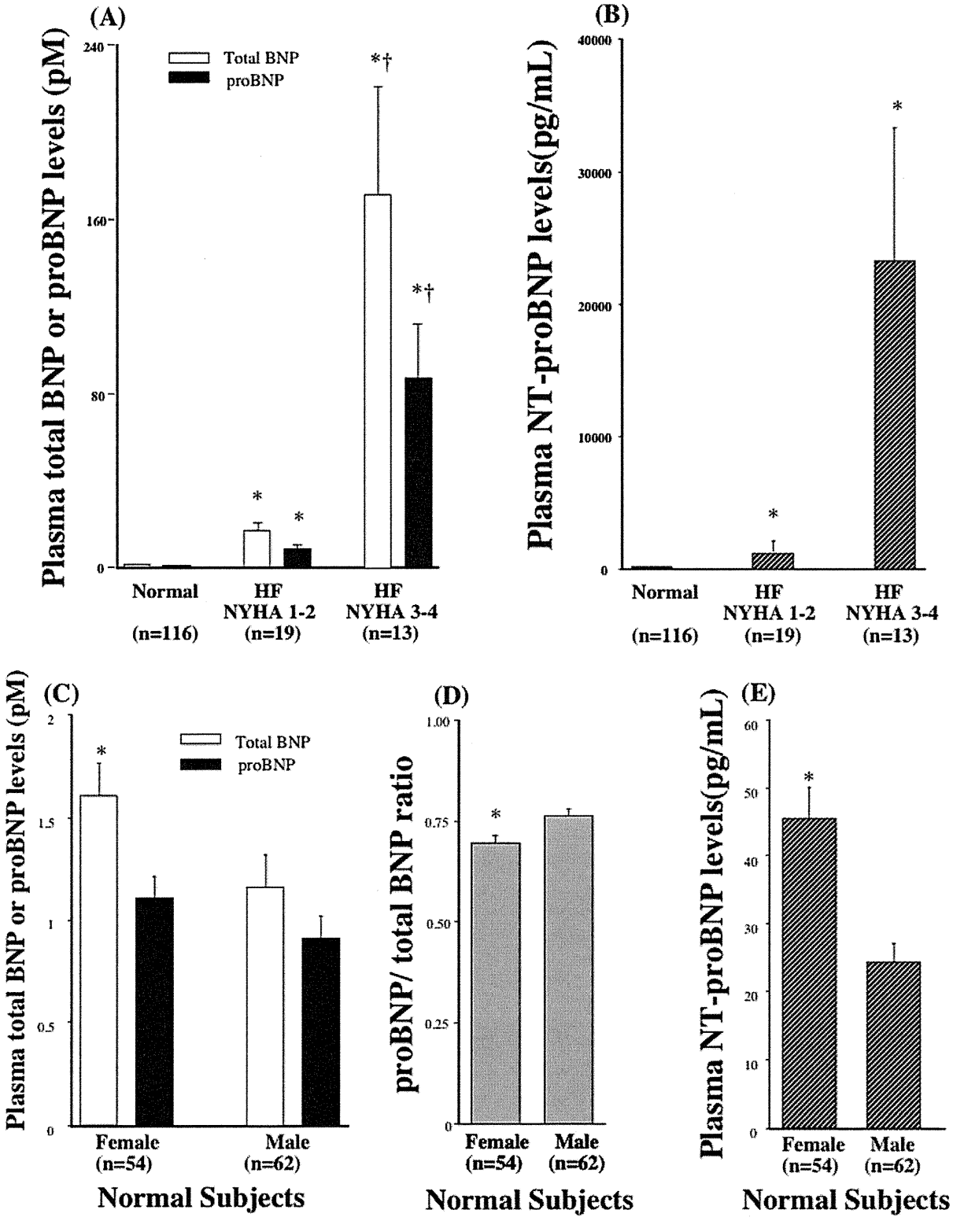

Figure 6. Plasma Levels of proBNP, total BNP, and NT-proBNP in normal and heart failure. Bar graph showing the total BNP, proBNP (A) and NT-proBNP (B) levels in healthy subjects and heart failure patients with NYHA classes 1–2 and 3–4. *P<0.05 vs total BNP and proBNP in normal, †P<0.05 vs total BNP and proBNP in HF NYHA 1–2. Bar graph showing the total BNP, proBNP (C), proBNP/total BNP ratio (D) and NT-proBNP (E) levels in male and female in healthy subjects. Values are means ± SE. *P<0.05 vs male.
doi:10.1371/journal.pone.0053233.g006

and a fluorescent immunoenzyme assay to measure BNP and proBNP, we found that levels of BNP were slightly higher than those of proBNP in both healthy subjects and heart failure patients. The exact reason for the discrepancy in proBNP levels between the earlier study and the present one is unclear; however, the lower recovery caused by the need for extraction from plasma on a Sep-Pak C18 cartridge may have contributed to the lower proBNP levels in the earlier study [9,16]. Recent studies have shown that proBNP has much less ability to induce cGMP production in vascular smooth muscle and endothelial cells than BNP [7,18]. This suggests that increases in the levels of the low-activity proBNP in heart failure may contribute to the so-called "BNP paradox" [19]. That is, administration of exogenous recombinant human BNP to heart failure patients has a substantial clinical and hemodynamic impact, despite the presence of high levels of immunoreactive BNP in their plasma, as measured with commercially used BNP assays.

In the current study, we showed that total BNP and NT-proBNP increased with aging, which are consistent with the previous studies. In addition, the current study first showed that plasma proBNP level increased with aging. However, there were no statistical differences in NT-proBNP between 30~39 and 50~59, whereas there were significant differences in total and proBNP between 30~39 and 50~59, suggesting that total and proBNP are more sensitive than NT-proBNP. In addition, total and proBNP seemed to be well correlated with age ($r = 0.467$. 0.491, each) than NT-proBNP ($r = 0.376$). Thus, total BNP and proBNP may be better marker in discriminating the effect of age than NT-proBNP. Increased myocardial mass and/or reduction of renal clearance of natriuretic peptides with aging may be one of the possible reason for increased BNP and NT-BNP with aging; however, exact mechanism for it still remains unknown and further study is necessary to investigate the relationships between proBNP and aging.

We also analyzed the effects of gender on proBNP, total BNP, proBNP/total BNP ratio and NT-proBNP. Interestingly, in female higher total BNP and NT-proBNP and lower proBNP/total BNP ratio without changing of proBNP was observed. Calculated BNP (total BNP - proBNP) was also increased. This finding may be explained that increased proBNP production and higher processing rate. Further study is necessary to elucidate the mechanism of increased total BNP and NT-proBNP and lower proBNP/total BNP ratio without changing of proBNP in female.

In summary, we have developed rapid and precise immunochemiluminescent assay systems for routine determination of total BNP and proBNP levels in human plasma. Using these assay systems we showed that in addition to BNP, considerable amount of proBNP circulates in both healthy subjects and heart failure patients. The precise relation of the proBNP/total BNP ratio to heart failure remains unknown, as does whether the heart mainly secretes proBNP. Likewise, the effects of age, sex and renal function on proBNP levels remain unknown. We anticipate our new assays for the proBNP and total BNP will be helpful for addressing each of those issues.

Acknowledgments

We thank Ms. Aoi Fujishima and Masako Matsubara for her excellent technical assistance and Ms.Yukari Kubo for her excellent secretarial work.

Author Contributions

Gave useful comments and discussion: K. Kamgawa K. Nakao. Conceived and designed the experiments: TN HO NM KH. Performed the experiments: MN NO K. Nagata. Analyzed the data: YN HK CY K. Nakao. Contributed reagents/materials/analysis tools: TM YK K. Koichiro IM. Wrote the paper: TN HO.

References

1. Maisel AS, Nakao K, Ponikowski P, Peacock WF, Yoshimura M, et al. (2011) Japanese-Western consensus meeting on biomarkers. Int Heart J. 52:253–65.
2. Jessup M, Abraham WT, Casey DE, Feldman AM, Francis GS, et al. (2009) ACCF/AHA Guidelines for the Diagnosis and Management of Heart Failure in Adults: a report of the American College of Cardiology Foundation/American Heart Association Task Force on Practice Guidelines: developed in collaboration with the International Society for Heart and Lung Transplantation. Circulation. 119:1977–2016.
3. Dickstein K, Cohen-Solal A, Filippatos G, McMurray JJ, Ponikowski P, et al. (2008) ESC Guidelines for the diagnosis and treatment of acute and chronic heart failure 2008: the Task Force for the Diagnosis and Treatment of Acute and Chronic Heart Failure 2008 of the European Society of Cardiology. Developed in collaboration with the Heart Failure Association of the ESC (HFA) and endorsed by the European Society of Intensive Care Medicine (ESICM). ESC Committee for Practice Guidelines (CPG). Eur Heart J. 29:2388–442.
4. Minamino N, Horio H, Nishikimi T (2006) Chapter 165. Natriuretic peptides in the cardiovascular system. In: Kastin AJ, editor. THE HANDBOOK OF BIOLOGICALLY ACTIVE PEPTIDES. 1st ed. Academic Press, pp. 1217–1225
5. Waldo SW, Beede J, Isakson S, Villard-Saussine S, Fareh J, et al. (2008) Pro-B-type natriuretic peptide levels in acute decompensated heart failure. J Am Coll Cardiol. 51:1874–82.
6. Nishikimi T, Minamino N, Ikeda M, Takeda Y, Tadokoro K, et al. (2010) Diversity of molecular forms of plasma brain natriuretic peptide in heart failure–different proBNP-108 to BNP-32 ratios in atrial and ventricular overload. Heart. 96:432–9.
7. Liang F, O'Rear J, Schellenberger U, Tai L, Lasecki M, et al. (2007) Evidence for functional heterogeneity of circulating B-type natriuretic peptide. J Am Coll Cardiol. 49:1071–8.
8. Nishikimi T, Minamino N, Horii K, Matsuoka H (2007) Do commercially available assay kits for B-type natriuretic peptide measure Pro-BNP1-108, as well as BNP1-32? Hypertension. 50:e163
9. Semenov AG, Seferian KR (2011) Biochemistry of the human B-type natriuretic peptide precursor and molecular aspects of its processing. Clin Chim Acta. 412:850–60
10. Tsuji T, Inouye K, Yamauchi A, Kono M, Igano K (2004) U.S. Patent 6, 677, 124 B2, pp 16, Shionogi Seiyaku Kabushiki Kaisha, Japan.
11. Seferian KR, Tamm NN, Semenov AG, Tolstaya AA, Koshkina EV, et al. (2008) Immunodetection of glycosylated NT-proBNP circulating in human blood. Clin Chem. 54:866–73.
12. Ishikawa E, Imagawa M, Hashida S, Yoshitake S, Hamaguchi Y, et al. (1983) Enzyme-labeling of antibodies and their fragments for enzyme immunoassay and immunohistochemical staining. J Immunoassay. 4:209–327.
13. Nishikimi T, Ikeda M, Takeda Y, Ishimitsu T, Shibasaki I, et al. (2012) The effect of glycosylation on plasma N-terminal proBNP-76 levels in patients with heart or renal failure. Heart. 98:152–61
14. Schellenberger U, O'Rear J, Guzzetta A, Jue RA, Protter AA, et al. (2006) The precursor to B-type natriuretic peptide is an O-linked glycoprotein. Arch Biochem Biophys. 451:160–6.
15. Nishikimi T, Kuwahara K, Nakao K. (2011) Current biochemistry, molecular biology, and clinical relevance of natriuretic peptides. J Cardiol. 57:131–40.
16. Seferian KR, Tamm NN, Semenov AG, Mukharyamova KS, Tolstaya AAet al. (2007) The brain natriuretic peptide (BNP) precursor is the major immunoreactive form of BNP in patients with heart failure. Clin Chem. 53:866–73.
17. Hammerer-Lercher A, Halfinger B, Sarg B, Mair J, Puschendorf B, et al. (2008) Analysis of circulating forms of proBNP and NT-proBNP in patients with severe heart failure. Clin Chem. 54:858–65.
18. Heublein DM, Huntley BK, Boerrigter G, Cataliotti A, Sandberg SM, et al. (2007) Immunoreactivity and guanosine 3′,5′-cyclic monophosphate activating actions of various molecular forms of human B-type natriuretic peptide. Hypertension. 49:1114–9.
19. Menon SG, Mills RM, Schellenberger U, Saqhir S, Protter AA (2009) Clinical implications of defective B-type natriuretic peptide. Clin Cardiol. 32:E36–41.

Heart Online First, published on October 31, 2012 as 10.1136/heartjnl-2012-302929

Complexity of molecular forms of B-type natriuretic peptide in heart failure

Toshio Nishikimi,[1] Koichiro Kuwahara,[1] Yasuaki Nakagawa,[1] Kenji Kangawa,[2] Naoto Minamino,[3] Kazuwa Nakao[1]

INTRODUCTION

In 1988, a Japanese group isolated B-type (or brain) natriuretic peptide (BNP) from porcine brain extracts by monitoring its relaxant effects on chick rectum.[1] Since then studies in humans and rodents demonstrated that BNP is a cardiac hormone mainly expressed in the heart, where its concentration is considerably higher than in brain. BNP possesses a 17-amino acid ring structure containing two cysteine residues, which is essential for its biological activity. Mechanical stress, ischaemia, cytokines and neurohumoral factors, including angiotensin II, stimulate expression of BNP (figure 1),[2] and levels of myocardial BNP mRNA and circulating BNP and N-terminal proBNP (NT-proBNP) are markedly increased in patients with congestive heart failure.[2] BNP is therefore considered to function as an emergency defence against ventricular overload in disease states.

MOLECULAR COMPLEXITY OF IMMUNOREACTIVE BNP IN HUMAN PLASMA

It is thought that human ProBNP is most likely cleaved by furin to BNP and NT-proBNP when it is secreted.[2] Once in the plasma, dipeptidyl peptidase IV removes the two N-terminal amino acids (Ser-Pro) of BNP to generate BNP[3–32], [3] the levels of which are increased in patients with heart failure.[4] Various BNP assay kits (eg, Shionogi, Biosite) similarly detect BNP[3–32] and BNP (figure 2).[5] In addition, other aminopeptidases may further digest the N-terminal region of BNP and/or BNP[3–32], and current assay systems likely also cross-react with these forms (figure 2). Consequently, the actual molecular forms of BNP circulating in plasma remain uncertain.

An early study failed to detect native BNP in plasma from New York Heart Association (NYHA) class-IV patients using solid phase extraction combined with liquid chromatography, immunodetection and mass spectrometry, despite BNP levels having been predetermined to exceed 1000 pg/ml. This suggests that native BNP may be altered in such patients.[6] Later attempts to quantify active BNP in the plasma of patients with heart failure using various extraction and detection methods, including mass spectrometry, detected BNP [3–32] in all patients along with other forms, including BNP[4–32], BNP[5–32], BNP[5–31], BNP[1–25] and BNP[1–26].[7] Incomplete protease inhibition during and after blood collection may partially explain why some investigators detected no BNP in the plasma of heart failure patients. However, when the sum of all the BNP breakdown products was measured in patients using mass spectrometry, it was verified to be only a small fraction of the total immunoreactive BNP determined using the Biosite assay,[7] which may be explained by antibody cross-reactivity with proBNP and related molecules (figure 2). A more recent study using mass spectrometry also confirmed the very low levels of biologically active BNP in the plasma of heart failure patients.[8] Moreover, clinical measurements of BNP made using an immunoassay correlated poorly with BNP levels measured using mass spectrometry, though they correlated well with BNP degradation fragments such as BNP[3–32], BNP[4–32] and BNP[5–32] (figure 2). These results suggest that clinically measured BNP includes numerous fragments that would be expected to have little compensatory biological activity. Whether molecular forms of BNP are altered in healthy individuals as well as in heart failure patients remains unknown. This is because measuring the subfractions of BNP metabolites is difficult in healthy individuals due to the low levels of BNP present.

These findings highlight the need for more specific clinical immunoassays to address the question of atypical proBNP processing and to accurately measure bioactive BNP concentrations. Mass spectrometry is thought to be a suitable technology for such studies.

PRESENCE OF proBNP IN BLOODSTREAM ASSOCIATED WITH HEART FAILURE

The clinical utility of BNP and NT-proBNP as biochemical markers of heart failure was established with BNP's original discovery as a cardiac hormone.[2] However, considerable uncertainty still surrounds the molecular forms of BNP. Earlier studies showing the presence of proBNP in human blood did not garner much attention, but recent studies have shown levels of proBNP to be higher than those of BNP in the plasma of heart failure patients.[9] In addition, one recent study further showed that both proBNP and BNP circulate in the plasma of heart failure patients, and that proBNP/BNP ratios vary widely depending on the heart failure status.[10]

All BNP assays, regardless of the source (eg, Shionogi, Biosite), cross-react with proBNP to some degree because the two antibodies used in the assays recognise epitopes common to BNP and proBNP (figure 2).[5] Whether the BNP values obtained with these assays indicate BNP, proBNP or their combination (BNP +proBNP) remains unknown, and the measured increases in plasma BNP levels seen in heart failure may reflect increases in proBNP as well as BNP. Similarly, all NT-BNP assays (regardless of source) cross-react with proBNP, but react little with glycosylated proBNP, as the attached *O*-saccharide almost completely inhibits antibody binding to the peptide.[11]

In vitro studies have shown that proBNP is much less able to induce guanosine 3′, 5′-cyclic monophosphate (cGMP) production in vascular smooth muscle and endothelial cells than BNP.[12] Plasma cGMP levels are increased in proportion to the severity of mild to moderate heart failure, and correlate with plasma BNP levels. However, the increases in cGMP are attenuated in patients with severe heart failure and a poor prognosis.[2] The observed increase in the levels of less

[1]Department of Medicine and Clinical Science, Kyoto University Graduate School of Medicine, Kyoto, Japan; [2]Department of Biochemistry, National Cerebral and Cardiovascular Center Research Institute, Osaka, Japan; [3]Department of Molecular Pharmacology, National Cerebral and Cardiovascular Center Research Institute, , Osaka, Japan

Correspondence to Professor Toshio Nishikimi, Department of Medicine and Clinical Science, Kyoto University Graduate School of Medicine, Shogoin-Kawara-cho 54, Sakyo-ku, Kyoto 606-8507, Japan; nishikim@kuhp.kyoto-u.ac.jp

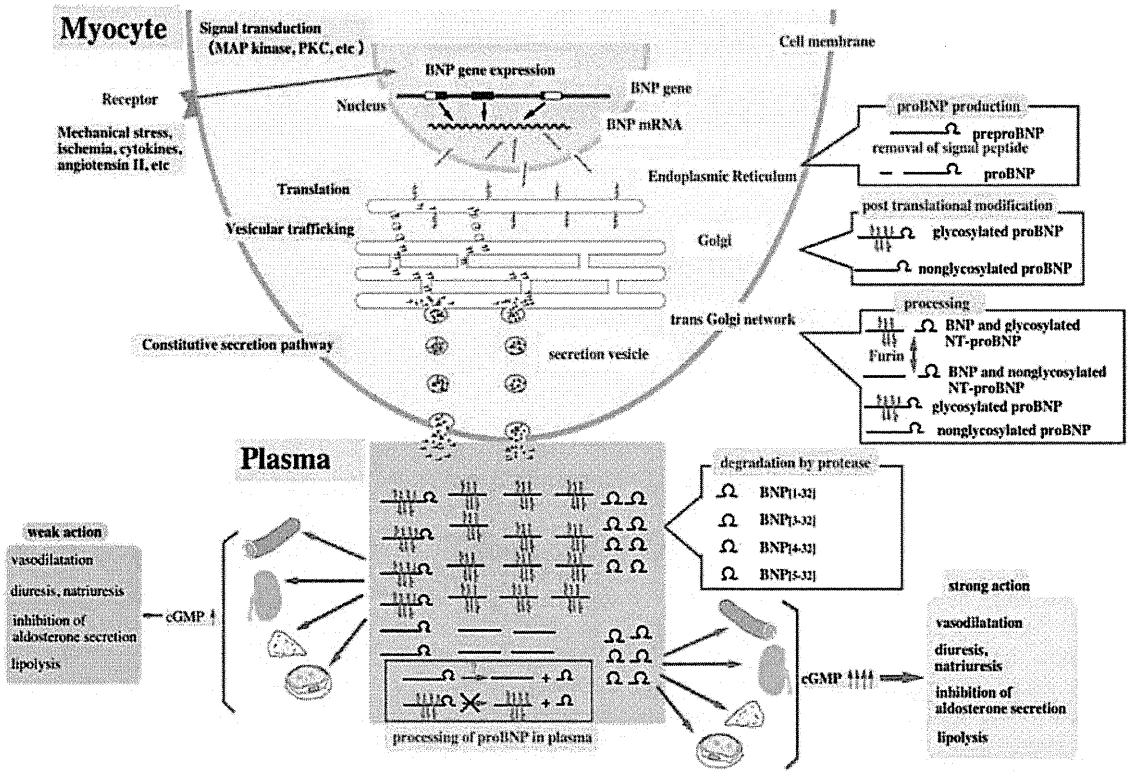

Figure 1 Schematic representation of the stimulus, signal transduction, gene, mRNA, translation, glycosylation, processing and secretion of B-type natriuretic peptide (BNP) in myocytes, and the plasma molecular forms of BNP. Mechanical stress, ischaemia, cytokines and neurohumoral factors (eg, angiotensin II and endothelin-1) stimulate gene expression of BNP via signal transduction mediated by protein kinase C and mitogen-activated protein (MAP) kinase. BNP mRNA is translated in the endoplasmic reticulum, after which preproBNP is converted to proBNP by a signal peptidase. ProBNP is post-translationally *O*-glycosylated within the Golgi apparatus and cleaved to BNP and NT-proBNP in equimolar fashion by furin within the trans-Golgi network. They are then transferred to secretion vesicles and secreted into the circulation via a so-called constitutive secretion pathway. ProBNP is often heavily *O*-glycosylated in the N-terminal region, and furin cannot easily cleave *O*-glycosylated proBNP when Thr71 is *O*-glycosylated. In the plasma, BNP is degraded to BNP [3-32] by dipeptidyl peptidase IV, after which BNP [3–32] is further degraded to BNP [4–32], BNP [5–32] and other metabolites by aminopeptidases. In addition, non-glycosylated proBNP may be processed into BNP and NT-proBNP by an unidentified mechanism, whereas glycosylated proBNP is not processed into BNP and NT-proBNP. BNP stimulates cGMP production via natriuretic peptide receptor-A in various tissues, including the vasculature, kidney, adrenal gland and adipose tissue, and induces vasodilation, diuresis, natriuresis, inhibition of aldosterone secretion and lipolysis. By contrast, glycosylated and non-glycosylated proBNP have little ability to stimulate cGMP production. Glycosylated and non-glycosylated NT-proBNP do not bind receptors and accumulate in the plasma in heart failure. This figure is only reproduced in colour in the online version.

hormonally active proBNP in severe heart failure may explain this phenomenon.[13] Indeed, one recent study showed that the proBNP/BNP ratio is increased in decompensated heart failure, and that medical therapy reduces plasma BNP and the patients' symptoms in concert with a reduction in the proBNP/BNP ratio in some cases.[10] Elucidation of the mechanism associated with the increased proBNP/BNP ratio should help to clarify the pathogenesis of heart failure and/or pave the way towards novel therapies.

PROBNP AND NT-proBNP ARE *O*-GLYCOSYLATED IN SEVERE HEART FAILURE

Not only do the levels of proBNP increase in heart failure, the degree to which proBNP is *O*-glycosylated also increases in proportion to heart failure severity.[13] Thus understanding the clinical relevance of proBNP glycosylation is a matter of obvious importance. Pressure and volume overload, ischaemia and other conditions stimulate BNP gene transcription.[2] BNP mRNA is translated in the endoplasmic reticulum to produce preproBNP. Subsequent removal of the signal peptide yields proBNP, which can be post-translationally glycosylated to varying degrees at several sites in its N-terminal region (Ser36, Thr37, Thr44, Thr48, Thr53, Ser58 and Thr71) while the protein is within the Golgi apparatus.[14] The *O*-glycosylated proBNP is transported to the trans-Golgi network, where it is cleaved to BNP and NT-proBNP by furin.[7] Both BNP and NT-proBNP are thought to be secreted via the constitutive secretion pathway without storage in secretory granules (figure 1).

Plasma levels of glycosylated proBNP, but not proBNP, are increased in patients with severe heart failure.[12] Why glycosylated proBNP is secreted without processing under conditions of severe heart failure is not fully understood at present. One recent study showed that *O*-glycosylation at Thr71 in a region close to the cleavage site impairs proBNP processing by furin in HEK293 cells.[15] But since the effect of *O*-glycosylation on furin-catalysed processing has only been evaluated in vitro, the roles of other possible processing enzymes remain unclear. In addition, whether these events occur in cardiac myocytes in the atria and/or ventricles also remains unknown. Further studies using cardiac myocytes will be required to clarify the precise mechanism of proBNP processing.

NT-proBNP is also *O*-glycosylated in heart failure.[11] An assay for NT-proBNP from Roche Diagnostics (Elecsys I) utilises polyclonal antibodies directed against epitopes proBNP[1–21] and proBNP[39–50], and monoclonal antibodies against epitopes proBNP[27–31] and proBNP[42–46]

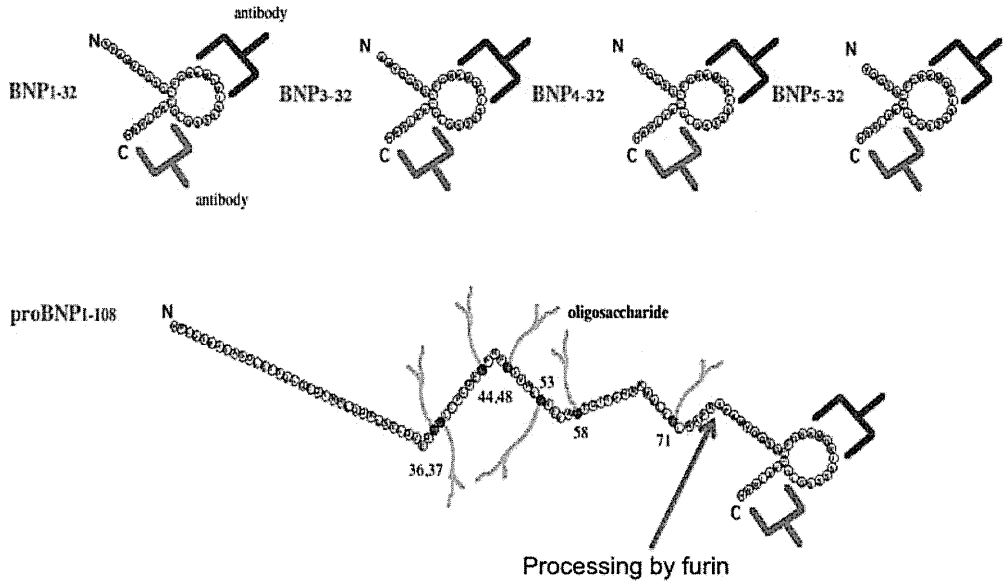

Figure 2 Schematic diagram illustrating the principle underlying the currently used B-type natriuretic peptide (BNP) assay systems. BNP is sandwiched by two antibodies. One is the capture antibody (red), and the other is the detection antibody (blue). This assay system measures BNP independently of the length of the N-terminal extension from the ring structure. Consequently, it cross-reacts with BNP[3–32], BNP[4–32], BNP[5–32] and proBNP[1–108]. This figure is only reproduced in colour in the online version.

have recently been introduced as Elecsys II. In both of these assays, glycosylation of the middle portion of NT-proBNP (Thr44, Thr48) could affect antibody binding (directed against proBNP[39–50] or proBNP[42–46]), potentially leading to an underestimation of the concentration of circulating NT-proBNP.[11] For example, measured levels of plasma NT-proBNP in heart failure increase fourfold to fivefold after enzymatic deglycosylation, as compared with glycosylated NT-proBNP.[11] On the other hand, numerous clinical studies have shown that the current NT-proBNP and BNP assays are equally valid for the diagnosis of heart failure. Therefore, an answer to whether new NT-proBNP assays using antibodies directed against non-glycosylated epitopes will result in better clinical applicability awaits further evaluation. Further studies will also be needed to identify the enzymes involved in the processing of non-glycosylated proBNP in the circulation and to determine how much non-glycosylated proBNP is actually present in human plasma.

CONCLUSION

Here we have briefly summarised the current understanding of the molecular forms of BNP. Several interesting issues remain to be addressed. It is therefore essential to unambiguously identify the molecular forms of BNP present in cardiac tissue and plasma. Also of importance is the relationship between the molecular forms of BNP in plasma and a patient's clinical condition. These studies may contribute not only to more accurate diagnosis of heart failure, but also to the clarification of the pathogenesis of heart failure and the development of new treatments.

Acknowledgements We thank Ms Aoi Fujishima (Kyoto University) for her excellent technical assistance and Ms Yukari Kubo (Kyoto University) for her excellent secretarial work.

Funding This study was supported in part by Scientific Research Grants-in-Aid 20590837 and 23591041 from the Ministry of Education, Culture, Sports, Science and Technology of Japan (to TN); a grant (AS 232Z01302F) from the Japan Science and Technology Agency (to TN); a grant from the Suzuken Memorial Foundation (to TN) and the Intramural Research Fund of National Cerebral and Cardiovascular Center (to NM).

Competing interests None.

Contributors TN mainly wrote the manuscript. YN, KK, and NM criticised it and provided the useful discussion.

KN and KK are supervisors and they provided useful comments to the manuscript.

Provenance and peer review Not commissioned; internally peer reviewed.

Heart 2012;**00**:1–3. doi:10.1136/heartjnl-2012-302929

REFERENCES

1. **Sudoh T,** Kangawa K, Minamino N, *et al*. A new natriuretic peptide in porcine brain. *Nature* 1988;**332**:78–81.
2. **Nishikimi T,** Kuwahara K, Nakao K. Current biochemistry, molecular biology, and clinical relevance of natriuretic peptides. *J Cardiol* 2011;**57**:131–40.
3. **Vanderheyden M,** Bartunek J, Goethals M, *et al*. Dipeptidyl-peptidase IV and B-type natriuretic peptide. From bench to bedside. *Clin Chem Lab Med* 2009;**47**:248–52.
4. **Lam CS,** Burnett JC Jr, Costello-Boerrigter L, *et al*. Alternate circulating pro-B-type natriuretic peptide and B-type natriuretic peptide forms in the general population. *J Am Coll Cardiol* 2007;**49**:1193–202.
5. **Heublein DM,** Huntley BK, Boerrigter G, *et al*. Immunoreactivity and guanosine 3′,5′-cyclic monophosphate activating actions of various molecular forms of human B-type natriuretic peptide. *Hypertension* 2007;**49**:1114–49.
6. **Hawkridge AM,** Heublein DM, Bergen HR III, *et al*. Quantitative mass spectral evidence for the absence of circulating brain natriuretic peptide (BNP-32) in severe human heart failure. *Proc Natl Acad Sci USA* 2005;**102**:17442–7.
7. **Niederkofler EE,** Kiernan UA, O'Rear J, *et al*. Detection of endogenous B-type natriuretic peptide at very low concentrations in patients with heart failure. *Circ Heart Fail* 2008;**1**:258–64.
8. **Miller WL,** Phelps MA, Wood CM, *et al*. Comparison of mass spectrometry and clinical assay measurements of circulating fragments of B-type natriuretic peptide in patients with chronic heart failure. *Circ Heart Fail* 2011;**4**:355–60.
9. **Waldo SW,** Beede J, Isakson S, *et al*. Pro-B-type natriuretic peptide levels in acute decompensated heart failure. *J Am Coll Cardiol* 2008;**51**:1874–82.
10. **Nishikimi T,** Minamino N, Ikeda M, *et al*. Diversity of molecular forms of plasma brain natriuretic peptide in heart failure—different proBNP-108 to BNP-32 ratios in atrial and ventricular overload. *Heart* 2010;**96**:432–9.
11. **Nishikimi T,** Ikeda M, Takeda Y, *et al*. The effect of glycosylation on plasma N-terminal proBNP-76 levels in patients with heart or renal failure. *Heart* 2012;**98**:152–61.
12. **Liang F,** O'Rear J, Schellenberger U, *et al*. Evidence for functional heterogeneity of circulating B-type natriuretic peptide. *J Am Coll Cardiol* 2007;**49**:1071–8.
13. **Hammerer-Lercher A,** Halfinger B, Sarg B, *et al*. Analysis of circulating forms of proBNP and NT-proBNP in patients with severe heart failure. *Clin Chem* 2008;**54**:858–65.
14. **Schellenberger U,** O'Rear J, Guzzetta A, *et al*. The precursor to B-type natriuretic peptide is an O-linked glycoprotein. *Arch Biochem Biophys* 2006;**451**:160–6.
15. **Semenov AG,** Postnikov AB, Tamm NN, *et al*. Processing of pro-brain natriuretic peptide is suppressed by O-glycosylation in the region close to the cleavage site. *Clin Chem* 2009;**55**:489–98.

Complexity of molecular forms of B-type natriuretic peptide in heart failure

Toshio Nishikimi, Koichiro Kuwahara, Yasuaki Nakagawa, et al.

Heart published online October 31, 2012
doi: 10.1136/heartjnl-2012-302929

The EMBO Journal (2012) 31, 4428–4440 | © 2012 European Molecular Biology Organization | All Rights Reserved 0261-4189/12
www.embojournal.org

THE EMBO JOURNAL

Reciprocal expression of MRTF-A and myocardin is crucial for pathological vascular remodelling in mice

Takeya Minami[1], Koichiro Kuwahara[1,*], Yasuaki Nakagawa[1], Minoru Takaoka[2], Hideyuki Kinoshita[1], Kazuhiro Nakao[1], Yoshihiro Kuwabara[1], Yuko Yamada[1], Chinatsu Yamada[1], Junko Shibata[1], Satoru Usami[1], Shinji Yasuno[3], Toshio Nishikimi[1], Kenji Ueshima[3], Masataka Sata[4], Hiroyasu Nakano[5], Takahiro Seno[6], Yutaka Kawahito[6], Kenji Sobue[7], Akinori Kimura[8], Ryozo Nagai[2] and Kazuwa Nakao[1]

[1]Department of Medicine and Clinical Science, Kyoto University Graduate School of Medicine, Kyoto, Japan, [2]Department of Cardiovascular Medicine, Graduate School of Medicine, The University of Tokyo, Tokyo, Japan, [3]EBM Research Center, Kyoto University Graduate School of Medicine, Kyoto, Japan, [4]Department of Cardiovascular Medicine, Institute of Health Biosciences, The University of Tokushima Graduate School, Tokushima, Japan, [5]Laboratory of Molecular and Biochemical Research, Department of Immunology, Biomedical Research Center, Juntendo University Graduate School of Medicine, Tokyo, Japan, [6]Department of Inflammation and Immunology, Graduate School of Medical Science, Kyoto Prefectural University of Medicine, Kyoto, Japan, [7]Department of Neuroscience, Institute for Biomedical Sciences, Iwate Medical University, Iwate, Japan and [8]Department of Molecular Pathogenesis, Medical Research Institute, Tokyo Medical and Dental University, Tokyo, Japan

Myocardin-related transcription factor (MRTF)-A is a Rho signalling-responsive co-activator of serum response factor (SRF). Here, we show that induction of MRTF-A expression is key to pathological vascular remodelling. MRTF-A expression was significantly higher in the wire-injured femoral arteries of wild-type mice and in the atherosclerotic aortic tissues of ApoE$^{-/-}$ mice than in healthy control tissues, whereas myocardin expression was significantly lower. Both neointima formation in wire-injured femoral arteries in MRTF-A knockout (*Mkl1*$^{-/-}$) mice and atherosclerotic lesions in *Mkl1*$^{-/-}$; *ApoE*$^{-/-}$ mice were significantly attenuated. Expression of vinculin, matrix metallopeptidase 9 (MMP-9) and integrin β1, three SRF targets and key regulators of cell migration, in injured arteries was significantly weaker in *Mkl1*$^{-/-}$ mice than in wild-type mice. In cultured vascular smooth muscle cells (VSMCs), knocking down MRTF-A reduced expression of these genes and significantly impaired cell migration. Underlying the increased MRTF-A expression in dedifferentiated VSMCs was the downregulation of microRNA-1. Moreover, the MRTF-A inhibitor CCG1423 significantly reduced neointima formation following wire injury in mice. MRTF-A could thus be a novel therapeutic target for the treatment of vascular diseases.

The EMBO Journal (2012) **31**, 4428–4440. doi:10.1038/emboj.2012.296; Published online 26 October 2012
Subject Categories: molecular biology of disease
Keywords: atherosclerosis; muscle, smooth; remodelling; signal transduction

Introduction

It is now recognized that modulation of vascular smooth muscle cell (VSMC) phenotypes plays a key role in the progression of several prominent cardiovascular disease states, including atherosclerosis, hypertension and restenosis (Schwartz *et al*, 1995; Owens *et al*, 2004). Pathological stress induces a switch from a differentiated VSMC phenotype, characterized by strong expression of contractile proteins and little capacity for migration or proliferation, to a proliferative dedifferentiated phenotype, characterized by relatively weak expression of contractile proteins and an increased capacity for migration and proliferation (Watanabe *et al*, 1999; Owens *et al*, 2004; Nishimura *et al*, 2006). VSMC proliferation and migration contribute to vascular remodelling and obstructive vasculopathies such as atherosclerosis and restenosis following percutaneous coronary intervention (Schwartz *et al*, 1995; Bentzon *et al*, 2006). Cytokines and growth factors locally secreted from cells within the vessel and infiltrating inflammatory cells induce migratory and proliferative responses in VSMCs during vascular remodelling (Owens *et al*, 2004), but the intracellular signalling pathways and the transcriptional regulators of phenotypic modulation of VSMCs are incompletely understood.

Myocardin, myocardin-related transcription factor (MRTF)-A (Mkl1, Bsac or Mal) and MRTF-B (Mkl2) are transcriptional cofactors that associate with serum response factor (SRF), an MADS box transcription factor and critical modulator of cardiovascular differentiation and growth, promoting transcription of a subset of genes involved in cytoskeletal organization and muscle differentiation (Wang *et al*, 2001, 2002; Miano, 2003; Olson and Nordheim, 2010). Myocardin, which is highly restricted to smooth and cardiac muscle cell lineages, is located constitutively in the nucleus and strongly activates transcription of SRF-regulated genes, thereby playing an important role in the differentiation and maintenance of cardiac and smooth muscle cell lineage. By contrast, MRTF-A and -B are expressed more ubiquitously and are found in both the cytoplasm and nucleus. In serum-starved fibroblasts, MRTF-A and -B are localized mainly in the cytoplasm and are translocated into the nucleus in response to stimulation with serum or other

*Corresponding author. Department of Medicine and Clinical Science, Kyoto University Graduate School of Medicine, 54 Shogoin Kawaharacho, Sakyo-ku, Kyoto 606-8507, Japan. Tel.: +81 75 751 4287; Fax: +81 75 771 9452; E-mail: kuwa@kuhp.kyoto-u.ac.jp

Received: 13 May 2012; accepted: 2 October 2012; published online: 26 October 2012

stimuli that promote Rho family GTPase activation and subsequent actin polymerization (Kuwahara *et al*, 2005; Nakamura *et al*, 2010; Olson and Nordheim, 2010). Thus, MRTF-A and -B transduce Rho family GTPase-actin signalling from the cytoplasm to SRF in the nucleus (Miralles *et al*, 2003).

Myocardin knockout leads to death *in utero* due to defects in vascular development (Li *et al*, 2003). In addition, myocardin mRNA levels have been shown to be downregulated in dedifferentiated VSMCs during vascular diseases (Liu *et al*, 2005; Chen *et al*, 2011). In contrast to myocardin, the roles played by MRTF-A in VSMC differentiation and phenotypic modulation remain unclear, though a recent human genetic analysis detected an association between coronary artery disease (CAD) and a single-nucleotide polymorphism (SNP) in the promoter region of the MRTF-A gene that enhances the gene expression (Hinohara *et al*, 2009). Li *et al* (2006) reported that MRTF-A knockout mice were born in anticipated Mendelian ratios, whereas Sun *et al* (2006) reported that MRTF-A knockout mice were born at less than the anticipated Mendelian ratio, which they attributed to fetal loss due to heart failure. In both groups, however, live born MRTF-A knockout pups showed no obvious gross abnormality or cardiovascular defect under normal conditions, except for a defect in maternal lactation due to impaired phenotypic modulation of mammary gland myoepithelial cells (Li *et al*, 2006; Sun *et al*, 2006).

In the present study, we investigated the potential roles of MRTF-A in the pathological processes underlying vascular proliferative diseases. We found that induction of MRTF-A expression is key to pathological remodelling underlying vascular disorders, as it sustains the SRF activity necessary for dedifferentiated VSMCs to acquire the capacity to migrate in response to extracellular stimuli. Our findings suggest that the reciprocal expression of MRTF-A and myocardin is mediated, at least in part, by microRNA (miR)-1 and contributes to the phenotypic modulation of VSMCs during vascular remodelling. These results point to MRTF-A as a potentially useful therapeutic target for the treatment of vascular diseases.

Results

Increased expression of MRTF-A in femoral arteries after wire injury

To explore the potential role played by MRTF-A during pathological vascular remodelling, we initially compared the expression of myocardin, MRTF-A and MRTF-B mRNA between femoral arteries subjected to wire injury or to a sham operation. As seen previously (Liu *et al*, 2005; Chen *et al*, 2011), levels of myocardin mRNA were significantly downregulated in femoral arteries 2 weeks after wire injury, while levels of MRTF-B mRNA were not significantly affected (Figure 1A). By contrast, expression of MRTF-A mRNA was significantly increased in injured arteries, as compared to sham-operated arteries (Figure 1A). Western blot analysis using specific antibodies for myocardin, MRTF-A and MRTF-B, respectively, clearly showed that the level of myocardin protein was reduced in injured arteries, whereas MRTF-A protein was significantly increased (Figure 1B and C; Supplementary Figure S1A). Immunohistochemical analysis showed that cells positively stained for MRTF-A were located mainly in the neointima of injured arteries (Figure 1D; Supplementary Figure S1B). Moreover, in serial sections stained for α-smooth muscle actin (αSMA) and smooth muscle myosin heavy chain (SM-MHC), most of the cells that positively stained for MRTF-A also positively stained for both αSMA and SM-MHC (Figure 1D). Time-course analysis of MRTF-A and myocardin expression revealed that MRTF-A mRNA levels were significantly increased by 2 weeks after injury, when dedifferentiated neointimal VSMCs expressing a relatively low level of αSMA were increasing (Shoji *et al*, 2004; Daniel *et al*, 2010). By 50 days after injury, when a more differentiated population of VSMCs is restored (Daniel *et al*, 2010), MRTF-A mRNA had declined to levels comparable to those seen on day 0 (Supplementary Figure S1C). By contrast, myocardin mRNA levels declined continuously for 2 weeks after injury, but had recovered by 50 days after injury (Supplementary Figure S1D). These results suggest that MRTF-A expression is upregulated in activated, dedifferentiated VSMCs during vascular remodelling, while myocardin expression is downregulated in these cells.

Attenuated vascular remodelling after wire injury in MRTF-A knockout mice

To further evaluate the function of MRTF-A during vascular remodelling, next we performed wire injury in the femoral arteries of MRTF-A knockout (*Mkl1*$^{-/-}$) mice. As previously reported, the *Mkl1*$^{-/-}$ mice were viable, fertile and showed no significant gross abnormalities or cardiovascular defects under normal conditions (Li *et al*, 2006). There was no difference in blood pressure or heart rate between wild-type and *Mkl1*$^{-/-}$ mice (Figure 2A), and the thickness of the medial wall in the uninjured sham-operated femoral arteries was comparable between wild-type and *Mkl1*$^{-/-}$ mice (Table I). Femoral arterial expression of myocardin mRNA was significantly weaker in *Mkl1*$^{-/-}$ mice 2 weeks after wire injury than in sham-operated arteries, just as was observed with wild-type mice (Figure 2B). On the other hand, neointima-to-medial ratios determined 4 weeks after wire injury were significantly smaller in *Mkl1*$^{-/-}$ mice than in wild-type mice, whereas there was no difference in medial thickness in the injured arteries between wild-type and *Mkl1*$^{-/-}$ mice (Figure 2C and D; Table I).

Four weeks after wire injury, the neointimal area comprised cells positively stained for αSMA was markedly smaller in *Mkl1*$^{-/-}$ mice than in wild-type mice (Figure 2D). Immunohistochemical analysis in serial sections stained for SM-MHC showed overlap with αSMA-positive cells (Figure 2D), suggesting that a reduction in the numbers of dedifferentiated VSMCs within the neointima is largely responsible for the reduction in the neointima-to-medial ratios seen in *Mkl1*$^{-/-}$ mice. Indeed, the numbers of Ki-67-positive proliferating cells within the injured vessels were also significantly lower in *Mkl1*$^{-/-}$ mice than in wild-type mice (Figure 2E and F). By contrast, the numbers of TUNEL-positive or cleaved caspase-3-positive apoptotic cells within the injured arteries did not differ between wild-type and *Mkl1*$^{-/-}$ mice (Supplementary Figure S2A through D). Similarly, the % fibrotic area in the media and intima and expression of the genes encoding collagen type 1 alpha1 and collagen type3 alpha1 within the injured arteries also did not significantly differ between wild-type and *Mkl1*$^{-/-}$ mice

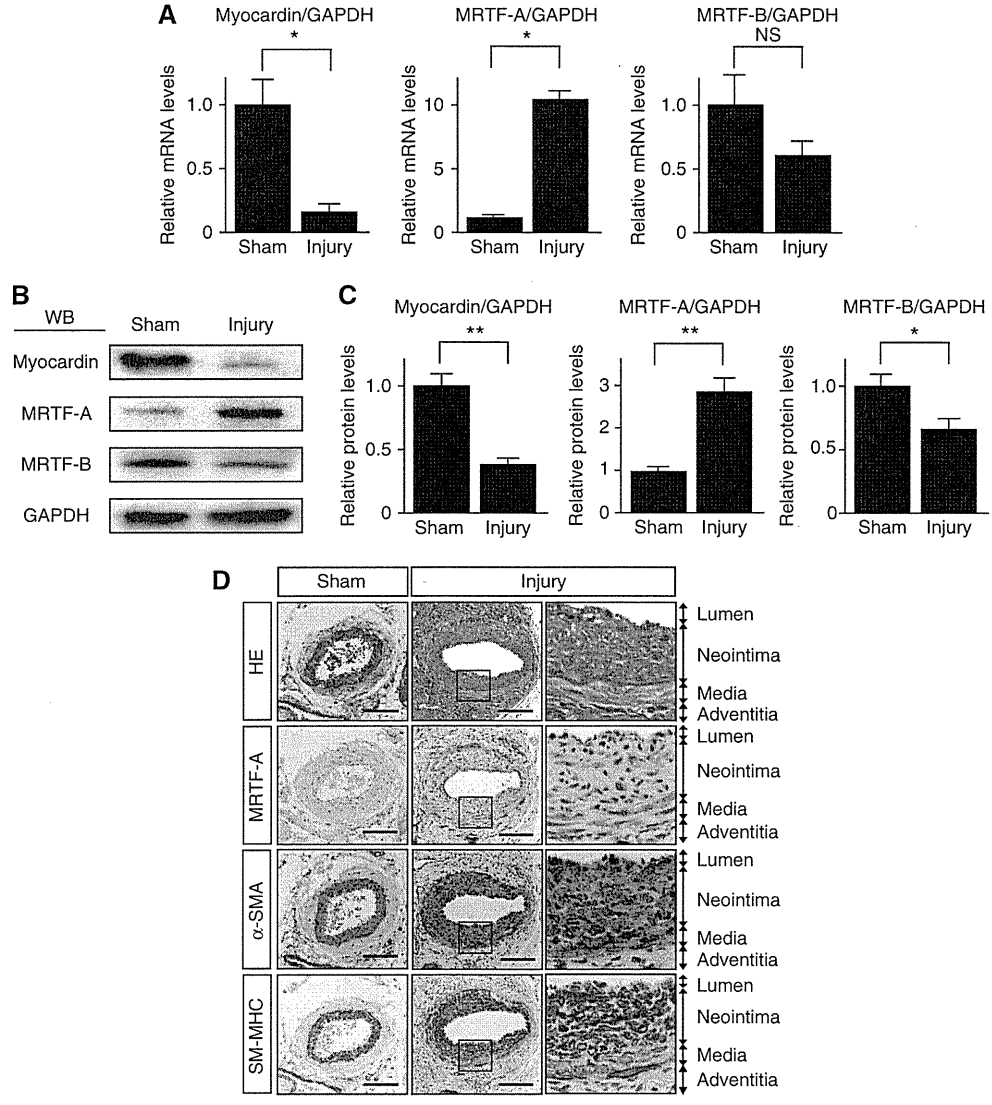

Figure 1 Increased expression of MRTF-A in femoral arteries after wire injury in mice. (**A**) Real-time RT–PCR analysis showing relative levels of myocardin, MRTF-A and MRTF-B mRNAs (normalized to GAPDH mRNA) in femoral arteries 2 weeks after wire injury (injury) ($n=6$ each). The relative mRNA level in sham-operated arteries (sham) was assigned a value of 1.0. (**B**) Representative western blots showing myocardin, MRTF-A and MRTF-B in wire-injured and sham-operated femoral arteries (2 weeks after injury). (**C**) The relative protein levels (normalized to GAPDH) of myocardin, MRTF-A and MRTF-B in wire-injured and sham-operated femoral arteries ($n=4$ each). The relative protein level in the sham-operated arteries was assigned a value of 1.0. (**D**) Immunohistochemical analysis of MRTF-A expression in sham-operated and wire-injured femoral arteries. Tissues are labelled with anti-BSAC (MRTF-A), anti-α-smooth muscle actin (αSMA) or anti-smooth muscle myosin heavy chain (SM-MHC) antibodies; bar indicates 100 μm. Three different experiments gave identical results. All graphs are shown as means ± s.e.m. $^*P<0.05$. $^{**}P<0.001$. NS, not significant. Figure source data can be found with the Supplementary data.

(Supplementary Figure S2E through G). In addition, because multiple cell types other than dedifferentiated VSMCs can contribute to neointima formation and to the vascular remodelling process, we also stained the tissue for endothelial cell (CD31) and macrophage (Mac3) markers. The relative numbers of CD31-positive and Mac3-positive cells in the injured arteries did not differ between wild-type and *Mkl1*$^{-/-}$ mice (Figure 2G through I), which indicates that a reduction in the number of αSMA-positive dedifferentiated VSMCs contributes to the attenuation of vascular remodelling in wire-injured *Mkl1*$^{-/-}$ mice. We also examined neointima formation following carotid artery ligation in *Mkl1*$^{-/-}$ mice, and found that neointima formation 4 weeks after carotid ligation was significantly diminished in *Mkl1*$^{-/-}$ mice, as compared to control *Mkl*$^{+/-}$ mice (Supplementary Figure S2H and I; Supplementary Table S1).

Loss of MRTF-A attenuates atherosclerotic lesions in APOE$^{-/-}$ *mice*

We next sought to analyse MRTF-A expression in a model of a different type of vascular disorder. *ApoE*$^{-/-}$ mice are prone to atherosclerotic lesions, to which both dedifferentiated VSMCs and infiltrating inflammatory cells contribute (Glass and Witztum, 2001; Bentzon *et al*, 2006). MRTF-A gene expression was significantly upregulated in aortic tissues containing atherosclerotic lesions in *ApoE*$^{-/-}$ mice fed a high cholesterol diet for 8 weeks (from 8 to 16 weeks of age), as compared to normal wild-type aortic tissues in

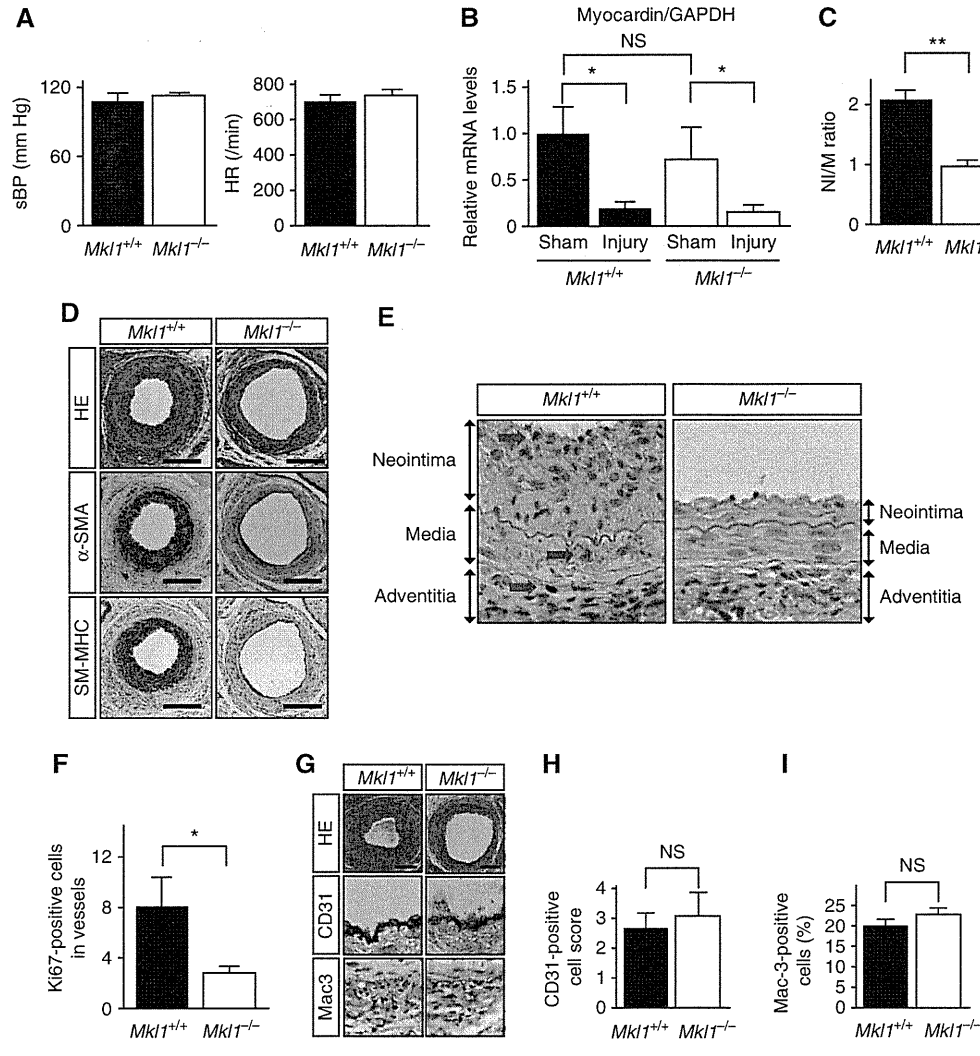

Figure 2 Attenuated vascular remodelling in response to wire injury in *Mkl1*$^{-/-}$ mice. (**A**) Systolic blood pressure (sBP) and heart rate (HR) in control *Mkl1*$^{+/+}$ and *Mkl1*$^{-/-}$ mice ($n=5$ each). (**B**) The relative levels of myocardin mRNA in wire-injured and sham-operated femoral arteries in *Mkl1*$^{+/+}$ and *Mkl1*$^{-/-}$ mice ($n=5$ each). (**C**) The neointima (NI)-to-media (M) ratio in arteries 4 weeks after wire injury in *Mkl1*$^{+/+}$ and *Mkl1*$^{-/-}$ mice ($n=20$ each). (**D**) Representative images of neointima in arteries 4 weeks after wire injury in *Mkl1*$^{+/+}$ and *Mkl1*$^{-/-}$ mice. HE: haematoxylin-eosin staining. α-SMA: staining with anti-α-SMA antibody. SM-MHC: staining with anti-SM-MHC antibody. (**E**) Representative images of neointima 4 weeks after femoral artery injury stained with anti-Ki-67 antigen in *Mkl1*$^{+/-}$ and *Mkl1*$^{-/-}$ mice. Red arrows indicate Ki-67-positive cells. (**F**) Numbers of Ki-67-positive cells in injured vessels of *Mkl1*$^{+/+}$ and *Mkl1*$^{-/-}$ mice 4 weeks after wire injury are shown ($n=3$ in each group). (**G**) Representative images of neointima stained with anti-CD31 (CD31) or anti-Mac3 (Mac3) antibody in arteries from *Mkl1*$^{+/+}$ and *Mkl1*$^{-/-}$ mice 4 weeks after wire injury. (**H, I**) The semi-quantitative CD31-positive scores ($n=5$ in each group) (**H**) and the relative numbers of Mac3-positive cells (% positive cells/total cells in neointima and media; $n=4$ in each group) (**I**) in *Mkl1*$^{+/+}$ and *Mkl1*$^{-/-}$ mice 4 weeks after wire injury are shown. All graphs are shown as means ± s.e.m. *$P<0.05$. **$P<0.001$. NS, not significant.

Table I Luminal and neointimal area of femoral arteries 4 weeks after vascular injury

	n	Lumen ($\times 10^3/\mu m^2$)	Intima ($\times 10^3/\mu m^2$)	Media ($\times 10^3/\mu m^2$)	IEL ($\times 10^3/\mu m^2$)	EEL ($\times 10^3/\mu m^2$)	Intima/Media ratio
Mkl1$^{+/+}$ sham	4	11.9 ± 2.7	0	19.0 ± 1.2	11.9 ± 2.7	30.9 ± 3.3	0
Mkl1$^{-/-}$ sham	4	10.4 ± 2.8	0	20.2 ± 2.5	10.4 ± 2.8	30.6 ± 2.8	0
Mkl1$^{+/+}$ injury	20	24.9 ± 3.5	39.7 ± 5.0	18.8 ± 1.1	64.8 ± 4.6	84.0 ± 5.4	2.09 ± 0.17
Mkl1$^{-/-}$ injury	20	29.6 ± 3.9	22.0 ± 2.3*	22.7 ± 1.2	52.3 ± 4.6	75.3 ± 5.3	0.96 ± 0.10*

The ratio of intima to media was calculated as the intimal area/medial area. Values are means ± s.e.m. IEL, internal elastic lamina; EEL, external elastic lamina. *$P<0.01$ versus *Mkl1*$^{+/+}$ injured arteries.

age-matched mice (Figure 3A). By contrast, myocardin gene expression was significantly decreased in atherosclerotic aortas, compared to normal aortas (Figure 3A). Consistent with that finding, cells positively stained for MRTF-A were observed within atherosclerotic lesions in the proximal aorta of *ApoE*$^{-/-}$ mice (Figure 3B).

To evaluate directly the contribution of MRTF-A to the development of atherosclerotic lesions in *ApoE*$^{-/-}$ mice, we crossed *Mkl1*$^{-/-}$ and *Apo E*$^{-/-}$ mice. Although the blood pressures, heart rates, cholesterol profiles and myocardin gene expression in aortic tissues did not differ between *Mkl1*$^{+/+}$;*ApoE*$^{-/-}$ and *Mkl1*$^{-/-}$;*ApoE*$^{-/-}$ mice

(Supplementary Figure S3A; Figure 3C), en-face analysis of the global progression of atherosclerotic lesions throughout the aorta revealed that the aortas of *Mkl1*$^{-/-}$;*ApoE*$^{-/-}$ mice contained smaller atherosclerotic lesions than those of *Mkl1*$^{+/+}$;*ApoE*$^{-/-}$ mice (Figure 3D). Furthermore, cross-sectional analysis of the proximal aorta revealed the average lesion area at the aortic root of *Mkl1*$^{-/-}$;*ApoE*$^{-/-}$ mice (2.5%) to be significantly smaller than at the aortic root of *Mkl1*$^{+/+}$; *ApoE*$^{-/-}$ mice (11.8%, $P<0.05$ versus *Mkl1*$^{-/-}$;*ApoE*$^{-/-}$) (Figure 3E and F). The relative accumulation of macrophages within atherosclerotic lesions at the aortic root, which was estimated based on the size of the

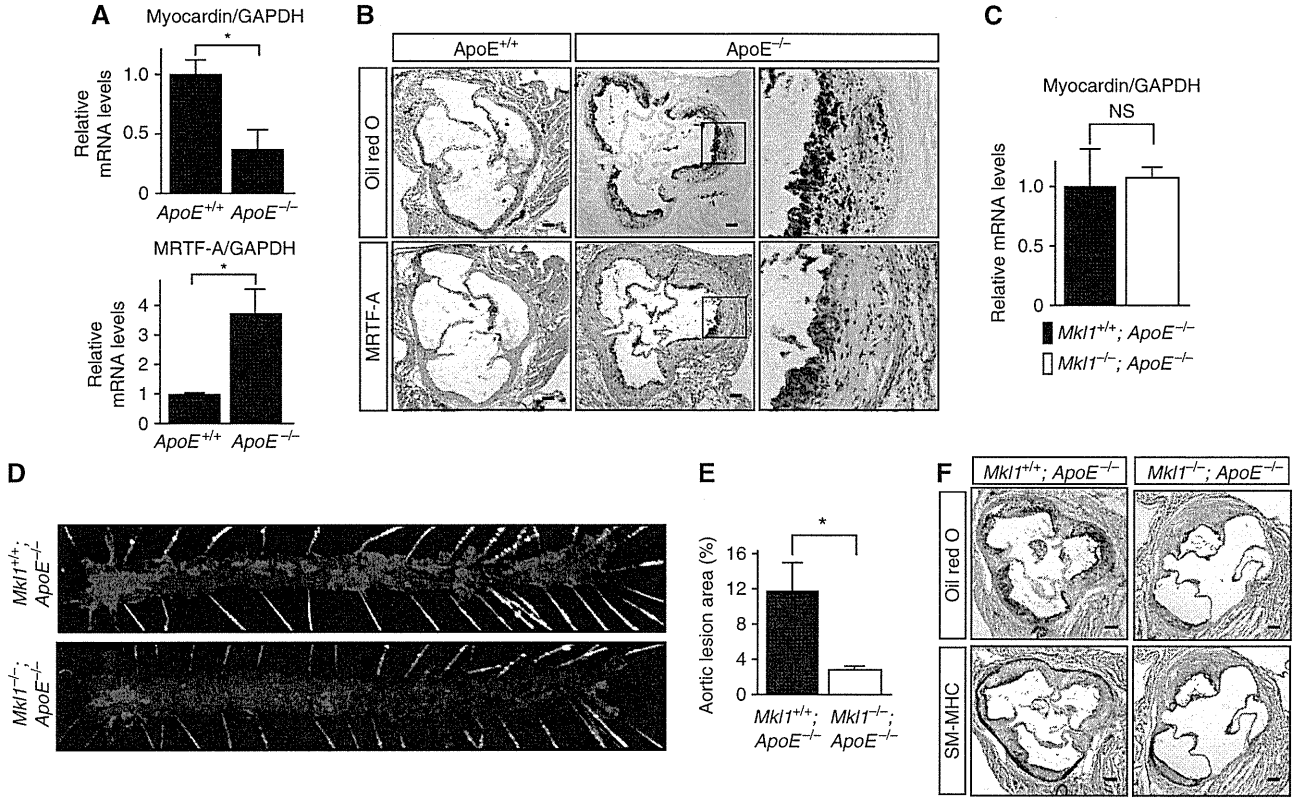

Figure 3 Atherosclerotic lesions in *Mkl1*$^{-/-}$;*ApoE*$^{-/-}$ mice are attenuated, as compared to those in *Mkl1*$^{+/+}$;*ApoE*$^{-/-}$ mice. (**A**) Real-time RT–PCR analysis showing the relative levels of MRTF-A and myocardin mRNAs (normalized to GAPDH mRNA) in atherosclerotic aortas from *ApoE*$^{-/-}$ mice fed a high-cholesterol diet and normal aortas from *ApoE*$^{+/+}$ mice at 16 weeks of age ($n=4$ each). *$P<0.05$. (**B**) Representative images showing MRTF-A expression within an atherosclerotic lesion in the proximal aorta of *ApoE*$^{-/-}$ mice. The tissues from *Apo*$^{+/+}$ and *ApoE*$^{-/-}$ mice were stained using anti-BSAC antibodies (MRTF-A). Oil-red O: Oil-red O staining. Three different experiments gave identical results. (**C**) Real-time RT–PCR analysis showing the relative levels of myocardin mRNA in atherosclerotic aortas from *Mkl1*$^{-/-}$;*ApoE*$^{-/-}$ and *Mkl1*$^{+/+}$;*ApoE*$^{-/-}$ mice fed a high-cholesterol diet ($n=4$ each). (**D**) Representative images of atherosclerotic lesions from an en-face analysis of the total aorta in *Mkl1*$^{+/+}$;*ApoE*$^{-/-}$ and *Mkl1*$^{-/-}$;*ApoE*$^{-/-}$ mice fed a high-cholesterol diet. Sudan III staining. Three independent experiments showed identical results. Red colour shows lipid-laden areas representing atherosclerotic lesions. (**E**) Graphs showing the relative (%) area of atherosclerotic lesions in cross-sections of proximal aorta from *Mkl1*$^{+/+}$;*ApoE*$^{-/-}$ and *Mkl1*$^{-/-}$;*ApoE*$^{-/-}$ mice fed a high-cholesterol diet for 8 weeks ($n=8$ each). *$P<0.05$. (**F**) Representative images of atherosclerotic lesions in cross-sections of proximal aorta from *Mkl1*$^{+/+}$;*ApoE*$^{-/-}$ and *Mkl1A*$^{-/-}$;*ApoE*$^{-/-}$ mice fed a high-cholesterol diet. Oil-red O: Oil-red O staining. SM-MHC: staining with anti-SM-MHC antibody. Bar indicates 100 μm. All graphs are shown as means ± s.e.m.

Figure 4 MRTF-A mediates acquisition of migration capacity by dedifferentiated VSMCs through regulation of SRF-target genes. (**A**) Real-time RT–PCR analysis showing relative levels of vinculin, MMP9 and integrin β1 mRNAs (normalized to GAPDH mRNA) in femoral arteries 2 weeks after wire injury in *Mkl1*$^{+/+}$ and *Mkl1*$^{-/-}$ mice ($n=4$ each). (**B**) Representative western blots showing myocardin, MRTF-A and MRTF-B in arteries 2 weeks after wire injury, in sham-operated arteries and in cultured mouse aortic VSMCs (MAVSMCs) and rat aortic VSMCs (RAVSMCs). (**C**) Real-time RT–PCR analysis showing the relative levels of myocardin, MRTF-A and MRTF-B mRNAs in femoral arteries 2 weeks after wire injury (injury), in sham-operated arteries (sham) and in cultured MAVSMCs and RAVSMCs ($n=6$ each). (**D**) Real-time RT–PCR analysis showing relative levels of MRTF-A, myocardin, vinculin, MMP9 and integrin β1 mRNAs in RAVSMCs transfected with MRTF-A siRNA or control siRNA ($n=6$ each). (**E**) Co-transfection of a plasmid expressing MRTF-A (0, 10 and 100 ng) plus the luciferase reporter gene driven by bp −360 to +63 of the 5′-flanking region of vinculin gene (vinculin-luc) into RAVSMCs (left panel) and NIH3T3 cells (right panel). Relative luciferase activities normalized to Renilla luciferase (pRL-TK) activity are shown. Vinculin CArG-mut-luc: luciferase reporter gene driven by the vinculin promoter harbouring a mutation within the CArG-box. Data were obtained from three experiments performed in sextuplicate. (**F**) Co-transfection of MRTF-A siRNA plus vinculin-luc into RAVSMCs. Relative luciferase activities normalized to Renilla luciferase activity are shown. Data were obtained from two experiments performed in sextuplicate. (**G**) Migration in the presence or absence of PDGF-BB of RAVSMCs transfected with MRTF-A siRNA or control siRNA. Data were obtained from three experiments performed in sextuplicate. (**H**) Proliferation in the presence or absence of fetal calf serum (FCS) of RAVSMCs transfected with MRTF-A siRNA or control siRNA. Data were obtained from three experiments performed in sextuplicate. All graphs are shown as means ± s.e.m. *$P<0.05$ and **$P<0.01$. NS, not significant. Figure source data can be found with the Supplementary data.

F4/80-stained area normalized to the corresponding total atherosclerotic lesion area, did not significantly differ between *Mkl1*$^{+/+}$;*ApoE*$^{-/-}$ and *Mkl1*$^{-/-}$;*ApoE*$^{-/-}$ mice (Supplementary Figure S3B).

MRTF-A is necessary for acquisition of migratory capacity in dedifferentiated VSMCs

SRF controls cellular migration capacity in various cell types, including dedifferentiated VSMCs, by regulating the expres-

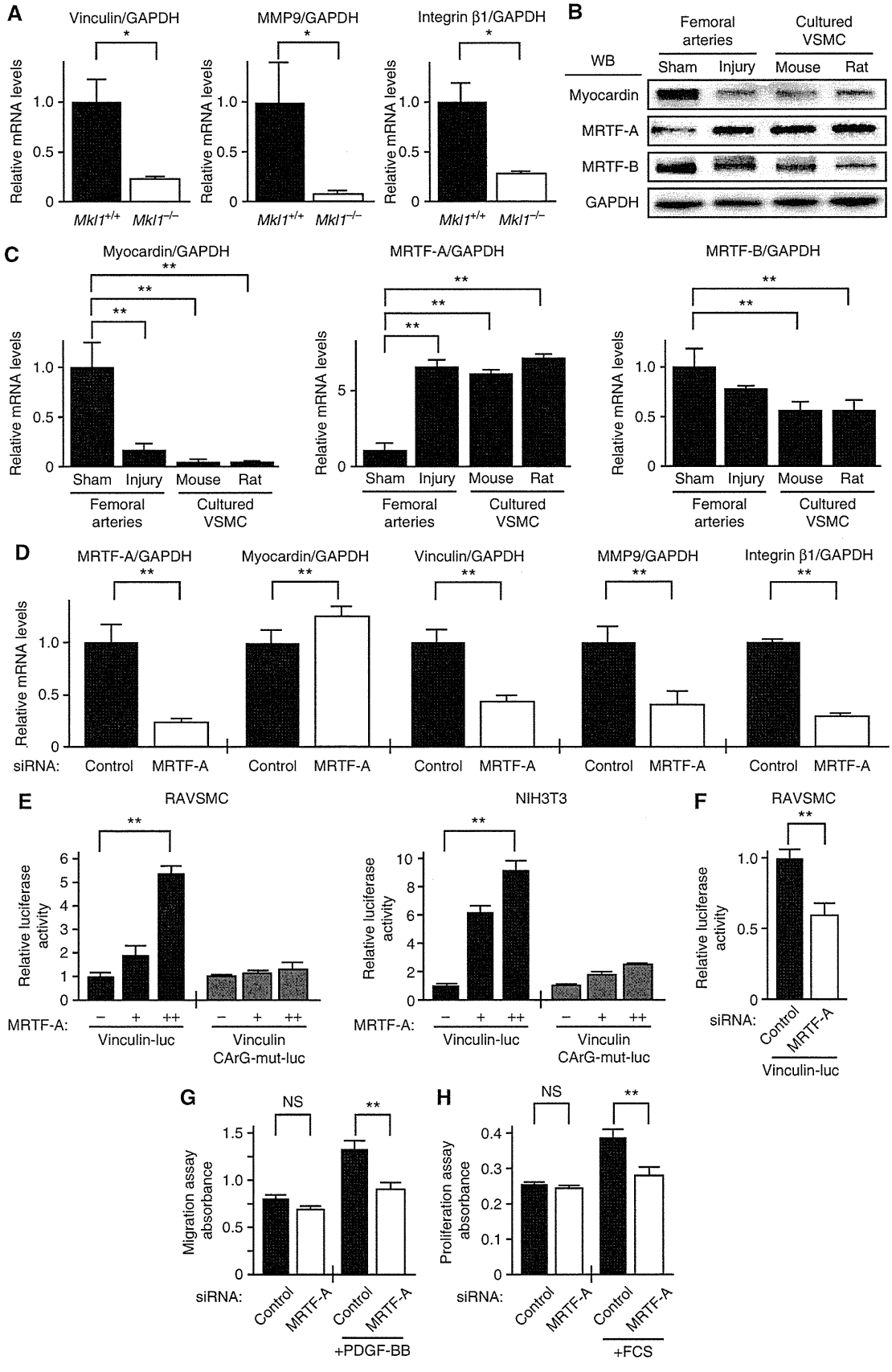

sion of several target genes, including the genes encoding vinculin, MMP9 and integrin β1 (Kenagy *et al*, 1997; Xu *et al*, 1998; Morita *et al*, 2007; Medjkane *et al*, 2009; Olson and Nordheim, 2010). We therefore examined the expression of these SRF-target genes in wire-injured femoral arteries. We found that 2 weeks after wire injury there was significantly less expression of vinculin, MMP9 and integrin β1 genes in the injured femoral arteries of $Mkl1^{-/-}$ mice than control $Mkl1^{+/+}$ mice (Figure 4A). The expression of these genes in the intact femoral arteries of $Mkl1^{-/-}$ and control $Mkl1^{+/+}$ mice was not significantly different (Supplementary Figure S4A). The mRNA expression of other SRF targets, αSMA (*ACTA2*) and SM-MHC (*Myh11*) genes encoding smooth muscle-specific contractile proteins, was also significantly less in the injured femoral arteries of $Mkl1^{-/-}$ mice than $Mkl1^{+/+}$ mice (Supplementary Figure S4B). In primary mouse aortic VSMCs (MAVSMCs), a cellular model of dedifferentiated VSMCs in which MRTF-A expression is increased and myocardin expression is decreased (Figure 4B and C; Supplementary Figure S4C; Hinson *et al*, 2007; Nakamura *et al*, 2010), levels of vinculin, MMP9, integrin β1 and αSMA mRNA were significantly reduced after knocking down MRTF-A (Figure 4D; Supplementary Figure S4D). This suggests that MRTF-A plays a predominant role in maintaining the expression of several SRF-target genes involved in cellular migration in dedifferentiated VSMCs, where expression of myocardin is decreased (Figure 4B and C; Nakamura *et al*, 2010). Overexpression of MRTF-A stimulated vinculin promoter activity in an SRF-dependent manner in both primary rat aortic VSMCs (RAVSMCs) and NIH3T3 fibroblasts (Figure 4E), whereas knocking down MRTF-A reduced vinculin promoter activity in RAVSMCs (Figure 4F). This supports the conclusion that MRTF-A regulates the expression of SRF-target genes in dedifferentiated VSMCs. Furthermore, knocking down MRTF-A significantly impaired PDGF-BB-induced RAVSMC migration, whereas knocking down myocardin did not (Figure 4G; Supplementary Figure S4E and F).

Because SRF is also known to control cellular proliferation, we examined the effect of MRTF-A knockdown on RAVSMC proliferation, and found that knocking down MRTF-A significantly reduced serum-induced RAVSMC proliferation, whereas knocking down myocardin did not (Figure 4H; Supplementary Figure S4G).

Reduced miR-1 expression contributes to the increase in MRTF-A expression in dedifferentiated VSMCs

We next investigated the molecular mechanisms potentially involved in regulating the reciprocal expression of MRTF-A and myocardin during VSMC dedifferentiation. We initially hypothesized that increased expression of myocardin leads to the repression of MRTF-A gene transcription through either direct or indirect mechanisms. Within the MRTF-A gene, the 5′-flanking region (FR) up to 1 kbp from the transcription start site is well conserved among different species. However, we failed to detect any significant effects of myocardin or MRTF-A on the activity of −930 bp MRTF-A promoter region in either RAVSMCs or NIH3T3 cells (Figure 5A; Supplementary Figure S5A). Myocardin also did not significantly affect the promoter activity of −5500 bp MRTF-A promoter region in either RAVSMCs or NIH3T3 cells (Supplementary Figure S5B). We therefore focused on the role of the 3′-untranslated region (UTR) of MRTF-A mRNA, where we found a conserved target site for microRNA-1 (miR-1) (Figure 5B). We observed that expression of miR-1 in vascular tissues is >100 times higher than in several non-muscle tissues, though its expression in skeletal and cardiac muscle tissues is much higher (Figure 5C). Consistent with earlier reports that miR-1 expression is regulated by myocardin and SRF in VSMCs and is downregulated in neointimal lesions created by ligation of carotid arteries of mice (Zhao *et al*, 2005; Chen *et al*, 2011), miR-1 expression was significantly weaker in the injured femoral arteries and atherosclerotic aorta of $ApoE^{-/-}$ mice, where there was a corresponding reduction of myocardin expression, than in control arteries (Figures 1A through C and 5D; Supplementary Figure S5C). Levels of miR-1 expression were also substantially lower in cultured RAVSMCs than in normal arteries (Supplementary Figure S5D). Overexpression of a miR-1 mimic significantly reduced endogenous MRTF-A gene and protein expression in RAVSMCs (Figure 5E and F), whereas overexpression of a miR-1 inhibitor significantly increased MRTF-A mRNA and protein expression (Figure 5G and H).

We also assessed miR-1-induced repression of MRTF-A gene by placing its 3′-UTR downstream of a cytomegalovirus (CMV)-driven luciferase reporter and performing luciferase assays in COS7 cells transfected with a miR-1 mimic or control scrambled oligo (Figure 5I). The miR-1 mimic significantly reduced the activity of the luciferase reporter linked to the MRTF-A 3′-UTR, and a mutation in the predicted miR-1 binding site in the 3′-UTR prevented that repression (Figure 5J). Moreover, overexpression of myocardin in A7r5 VSMCs significantly repressed the activity of a luciferase reporter gene linked to the MRTF-A 3′-UTR in a miR-1-dependent fashion (Figure 5K). These results strongly suggest that reduced expression of miR-1 caused by the reduction in myocardin expression during the process of phenotypic modulation of VSMCs contributes to the increase in MRTF-A expression in dedifferentiated VSMCs. Consistent with those findings, injection of an anti-miR-1 Locked Nucleic Acid (LNA)™-enhanced microRNA inhibitor into the injured vessels led to an increase in MRTF-A gene expression and exacerbated the pathological vascular remodelling after wire injury (Supplementary Figure S5E through G; Supplementary Table S2).

Pharmacological inhibition of MRTF-A activity attenuates adverse vascular remodelling after wire injury

The results presented raise the possibility that MRTF-A is a novel therapeutic target for the treatment of vascular disease. Recently, a small molecule (CCG-1423) was found to inhibit Rho pathway-mediated SRF activation (Evelyn *et al*, 2007; Jin *et al*, 2011). CCG-1423 appears to inhibit the interaction between SRF and MRTF-A at a point upstream of the DNA binding. Although the site of inhibition and its selectivity is not yet precisely defined, it was recently shown that CCG-1423 blocks nuclear translocation of MRTF-A, thereby inhibiting MRTF-A-mediated effects on SRF transcription, at least in part (Jin *et al*, 2011). In addition, we confirmed that CCG-1423 blocks serum-induced nuclear accumulation of endogenous MRTF-A in RAVSMCs (Figure 6A). CCG-1423 also significantly blocked SRF activity induced by co-expres-

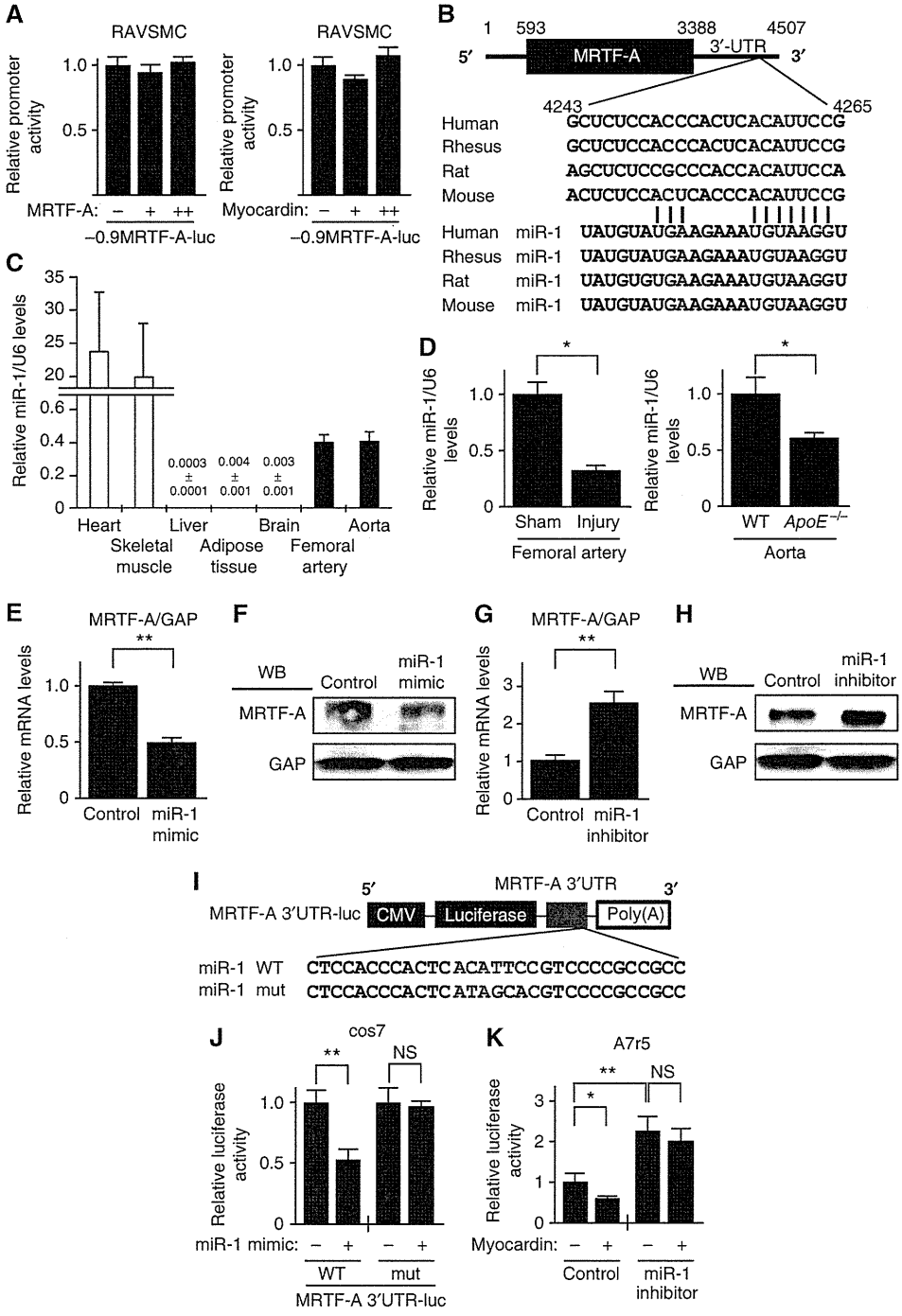

Figure 5 MicroRNA-1 regulates MRTF-A gene expression. (**A**) Co-transfection of a plasmid encoding myocardin or MRTF-A (0, 10 and 100 ng) with the −930 bp MRTF-A-luc gene into RAVSMCs. Data were obtained from two experiments performed in quadruplicate. +: 10 ng. ++: 100 ng. (**B**) Schematic representation of the MRTF-A 3′-untranslated region (UTR) containing a conserved microRNA-1 (miR-1) target site (shown in red). Sequences of mature miR-1 in different species are shown below. (**C**) Real-time RT–PCR analysis showing the relative miR-1 expression (normalized to the U6 levels) in different mouse tissues. (**D**) Real-time RT–PCR analysis showing the relative miR-1 expression (normalized to the U6 levels) in femoral arteries 2 weeks after wire injury or sham operation in wild-type mice ($n=4$ each) (left panel), and in aortic tissues in *ApoE*$^{-/-}$ or control wild-type mice (right panel). (**E**) Endogenous expression of MRTF-A mRNA in RAVSMCs transfected with miR-1 mimic or control oligo. Graphs show the relative MRTF-A mRNA levels (normalized to GAPDH mRNA) ($n=4$ each). (**F**) Representative western blots showing the effect of miR-1 mimic on MRTF-A expression in RAVSMCs. Three different experiments gave identical results. (**G**) Endogenous MRTF-A mRNA expression in RAVSMCs transfected with miR-1 inhibitor. Graphs show the relative MRTF-A mRNA levels ($n=4$ each). (**H**) Representative western blots showing the effect of a miR-1 inhibitor on MRTF-A expression in RAVSMCs. Three different experiments gave identical results. (**I**) Luciferase reporter constructs containing wild-type and mutant MRTF-A 3′UTR (MRTF-A 3′UTR-luc and mutMRTF-A 3′UTR-luc, respectively). The conserved miR-1 target site is shown in red. In mutMRTF-A 3′UTR-luc, mutations were introduced within the miR-1 target site (shown in blue). (**J**) MRTF-A 3′UTR-luc and mutMRTF-A 3′UTR-luc were co-transfected with miR-1 mimic into COS7 cells for 48 h. Data were obtained from three experiments performed in quadruplicate. (**K**) MRTF-A 3′UTR-luc was transfected with or without a plasmid expressing myocardin and/or a miR-1 inhibitor into A7r5 cells for 48 h. Data were obtained from three experiments performed in quadruplicate. All graphs are shown as means ± s.e.m. Relative luciferase activities normalized to control Renilla luciferase activity are shown. *$P<0.05$. **$P<0.01$. NS, not significant. Figure source data can be found with the Supplementary data.

sion of striated muscle activator of rho signalling (STARS) and MRTF-A in RAVSMCs (Figure 6B; Kuwahara *et al*, 2005). STARS is an actin-binding protein that activates SRF by inducing nuclear accumulation of MRTF-A. Both CCG-1423 and MRTF-A knockdown similarly inhibited STARS-induced activation of SRF in RAVSMCs. Furthermore, this inhibitory effect of CCG-1423 on STARS-induced activation of SRF was abolished by knocking down MRTF-A, supporting the notion that CCG-1423 blocks MRTF-A-mediated activation of SRF (Supplementary Figure S6A) Similarly to knocking down MRTF-A, CCG-1423 significantly reduced the migration and proliferation capacities of RAVSMCs (Figure 6C and D). When we then treated mice subjected to femoral artery wire injury with CCG-1423 (0.15 mg/kg intraperitoneally for 3 weeks), we found that CCG-1423 significantly attenuated the progression of vascular remodelling in arteries 3 weeks after injury (Figure 6E and F; Table II; Supplementary Figure S6B and C), without affecting the hemodynamic parameters or cholesterol profiles (Supplementary Figure S6D and E). CCG-1423 did not affect gross appearance, body weight or survival among the mice during the experiment (data not shown). Furthermore, administration of CCG-1423 also significantly attenuated the